Nested sampling for Fully Bayesian Unfolding (PENDING TITLE)

by

Jens Bratten Due

THESIS

for the degree of

MASTER OF SCIENCE

Faculty of Mathematics and Natural Sciences

University of Oslo

June 2021

Abstract

This here is the abstract

Acknowledgements

Contents

Introduction

1 Introduction

Part I

Theory

Bayesian statistics

> Probability theory is nothing
> but common sense reduced to
> calculation.
>
> ———————————
> Pierre-Simon Laplace [1]

Sivias book *Data Analysis - a Bayesian tutorial* [1] is a great read, and provides the theoretical foundation for the majority of topics discussed in this SECTION/CHAPTER.

1   Bayes' theorem

First, we consider probability theory and its basic algebra which includes the sum rule

$$P(X|I) + P(\overline{X}|I) = 1 \tag{2.1}$$

and the product rule

$$P(X,Y|I) = P(X|Y,I) \times P(Y|I). \tag{2.2}$$

Here P stands for probability, the bar "|" means "given" and $\overline{X}$ means "not X". Lastly, we have the symbol I, meaning all relevant background information. The sum rule can then be stated as "the probability of X being true plus the probability of X not being true, both given all relevant background, equals 1".

Using the product rule, and the fact that $P(X,Y|I) = P(Y,X|I)$ we get the following.

$$P(X|Y,I) \times P(Y|I) = P(Y|X,I) \times P(X|I)$$

Rearranging this leads to *Bayes' theorem*

$$P(X|Y,I) = \frac{P(Y|X,I) \times P(X|I)}{P(Y|I)} \tag{2.3}$$

To get a clearer picture of the significance of Bayes' theorem, we can replace X and Y with *hypothesis* and *data*. $P(hypothesis|data,I)$ is then given the formal name *posterior probability*, $P(data|hypothesis,I)$ is called the *likelihood function* and $P(hypothesis|I)$ is called the *prior probability*, representing our knowledge about the truth of the hypothesis before any data has been analysed. The term in the denominator, $P(data|I)$, often called the *evidence*, is in many cases not shown, due to it often being absorbed by a normalization constant. We can then replace the equality sign with a proportionality.

$$P(hypothesis|data,I) \propto P(data|hypothesis,I) \times P(hypothesis|I) \tag{2.4}$$

In summary, Bayes' theorem describes a learning process, showing how a probability is augmented by the introduction of data.

Another useful result from using the sum and product rule is the *marginalization* equation

$$P(X|I) = \int_{-\infty}^{\infty} P(X,Y|I)dY \tag{2.5}$$

with a normalization condition

$$\int_{-\infty}^{\infty} P(Y|X,I)dY = 1. \tag{2.6}$$

The marginalization equation gives us the ability to integrate out so-called nuisance parameters, values of no interest to a specific problem, such as background signals and measurement byproducts. These rules of probability are widely applicable and provide a strong foundation for tackling data analysis problems. [1]

2   Parameter estimation I

We will now look at the act of estimating a single parameter using Bayes' theorem, such as the mass of a planet, or the charge of the electron. We will firstly go through the example of deducting the fairness of a coin. This can be represented by the *bias-weighting H*. $H = 1/2$ will mean the coin is fair, while $H = 1$ and $H = 0$ means the coin is showing only heads or tails every flip. This value is continuous on the range $[0,1]$, and $P(H|\{data\},I)$ describes

how much we believe H to be true. For a range of H-values, $P(H|\{data\}, I)$ is a *probability density function* (pdf). To find this, we use Bayes' theorem.

$$P(H|\{data\}, I) \propto P(\{data\}|H, I) \times P(H|I) \tag{2.7}$$

We can, if needed, find the normalization constant using equation (2.6). To express ultimate ignorance, we can assign a flat pdf for the prior.

$$P(H|I) = \begin{cases} 1 & 0 \leq H \leq 1 \\ 0 & \text{otherwise} \end{cases} \tag{2.8}$$

meaning we assume every value of H to be equally probable. Assuming each flip is an independent event, the likelihood function takes the form of the binomial distribution.

$$P(\{data\}|H, I) \propto H^R (1 - H)^{N-R} \tag{2.9}$$

where R is the number of heads and N is the number of flips.

    Plugging (8) and (9) into Bayes' theorem results in the posterior probability, the shape of which varies significantly for the first few data points. When the number of data increases however, the pdf becomes sharper and converges to the most likely value. The choice of prior becomes mostly irrelevant when we have a large of number of data, as the majority of propositions will converge to the same solution, but the speed of convergence may vary. A very confident, but wrong prior will often approach the correct solution more slowly than an ignorant one.

2.1   Reliabilities: best estimates, error-bars and confidence intervals

One way to summarize the posterior pdf is with two quantities: the best estimate and its reliability. The best estimate is given by the maximum value of the pdf

$$\left. \frac{dP}{dX} \right|_{X_O} = 0 \tag{2.10}$$

where X_O denotes the best estimate. To make sure we have a maximum, we also need to check the second derivative

$$\left. \frac{d^2 P}{dX^2} \right|_{X_O} < 0. \tag{2.11}$$

Using derivatives like this assumes X is continuous. If this is not the case, the best estimate will still be the value corresponding to the max of the pdf.

The reliability of the best estimate is found by considering the width of the pdf about X_O. We take the logarithm of the pdf as this varies more slowly with X, making it easier to work with.

$$L = ln[P(X|\{data\}, I)]. \tag{2.12}$$

Doing a Taylor expansion about X_O and using the condition

$$\left. \frac{dL}{dX} \right|_{X_O} = 0, \tag{2.13}$$

which is equivalent to (10), leads to

$$P(X|\{data\}, I) \approx A \exp \left[\frac{1}{2} \frac{d^2 L}{dX^2} \right|_{X_O} (X - X_O)^2 \right]. \tag{2.14}$$

Here, we only show the dominating quadratic term of the expansion, with A being a normalization constant. We have now approximated our pdf by the *normal distribution*, typically taking the form

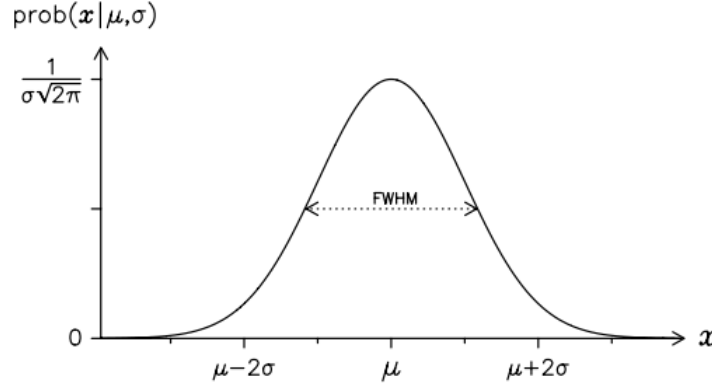$$P(x|\mu, \sigma) = \frac{1}{\sigma \sqrt{2\pi}} \exp \left[- \frac{(x - \mu)^2}{2\sigma^2} \right] \tag{2.15}$$

Figure 2.1: The normal distribution with a maximum at $x = \mu$ and a full width at half maximum (FWHM) of 2.35σ. (Sivia, 2006, p. 22) [1]

The parameter σ is called the *error-bar* and is defined as

$$\sigma = \left(- \frac{d^2 L}{dX^2} \right|_{X_O} \right)^{-1/2}. \tag{2.16}$$

We then infer the quantity of interest by the following

$$X = X_O \pm \sigma. \tag{2.17}$$

By calculating the integral of the normal distribution in this range, we get a 67% chance that X lies within $X_O \pm \sigma$ and a 95% chance that it lies within $X_O \pm 2\sigma$.

2.1.1 Asymmetric pdfs

The error-bar needs a symmetric pdf to be valid, something that is often not the case. This is solved by replacing the error-bar with a *confidence interval* as a measure of reliability. It is defined as the shortest interval that encloses 95% of the area of the pdf. In short, we find X_1 and X_2 such that

$$P(X_1 \leq X \leq X_2|\{data\}, I) = \int_{X_1}^{X_2} P(X|\{data\}, I)dX \approx 0.95, \tag{2.18}$$

assuming the pdf is normalized. The 95% confidence level is conventionally seen as a sensible value, being a rather conservative estimate.

In the case of an asymmetric pdf, we may consider using the *mean* or *expectation* as the best estimate. This quantity takes the skewness of the pdf into account, and is given by

$$\langle X \rangle = \int XP(X|\{data\}, I)dX. \tag{2.19}$$

If the pdf is not normalized, we also need to divide the right-hand side by $\int P(X|\{data\}, I)dX$.

If the pdf is *multimodal*, meaning it has multiple maxima, it becomes more difficult to calculate a best estimate and its reliability. If one maximum is much greater than the others, we can ignore those other contributions and focus on the largest. However, if multiple peaks are of similar size, we would be better off displaying the pdf itself.

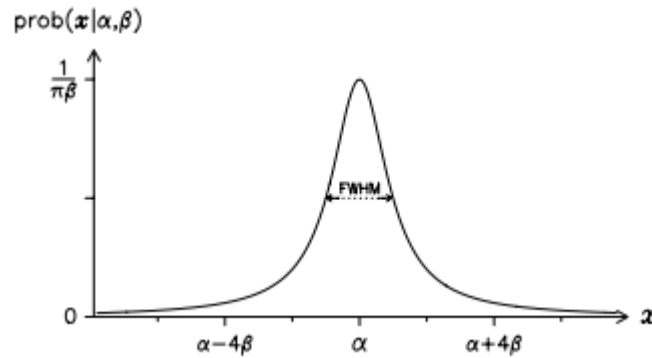Another common pdf which is often used is the Cauchy distribution, shown below.

Figure 2.2: The Cauchy distribution, symmetric about $x = \alpha$ and has a FWHM of 2β. (Sivia, 2006, p. 31) [1]

This distribution has very wide wings and is in this case given by

$$P(x|\alpha, \beta, I) = \frac{\beta}{\pi[\beta^2 + (x - \alpha)^2]} \tag{2.20}$$

Part II

Methods

Unfolding Methods

1 What is unfolding (maybe in Theory-chapter?)

- The inverse problem $f = Ru$

- The physics behind?

- The detector/experimental setup

- SiRi, OSCAr

- The raw data matrix, how it is produced?

1.1 The Response Matrix

The response matrix contains what we know about the circumstances of the experiment, a large part of which are the characteristics of the detector. The response matrix has elements given by:

$$R_{tr} = P(\text{reconstructed in bin r} \mid \text{true in bin t}) \tag{3.1}$$

[2]. This can be read as the probability of observing an event in energy bin r, given the true event happening in bin t. In a nutshell, the response matrix describes how a signal is smeared over the other bins in the spectrum.

- Multiplying with R^{-1} leads to fluctuations because we cannot assume the observed data equals the *expectation values* for the data. Statistical fluctuations in the data is assumed to come from a real structure in the true spectrum and will be magnified. http://www-library.desy.de/preparch/desy/proc/proc14-02/P52.pdf

2 The Folding Iteration Method

The following section describes the methods developed by Guttormsen et al. [3].

The folded spectrum f is on the form

$$f = \boldsymbol{R}u, \tag{3.2}$$

HAVE TO SWITCH AROUND TRUTH AND RECO BINS FOR THE ABOVE TO BE COR-RECT, I BELIEVE where $\boldsymbol{R}$ is the response matrix and u is the expectation values for the true spectrum. The iterative method can then be described in 4 parts.

- First we use the observed spectrum $\boldsymbol{D}$ as an initial guess,
  $u_0 = \boldsymbol{D}$

- We then fold this with the response matrix,
  $f_0 = \boldsymbol{R}u_0$

- The difference between the folded and the raw spectrum is calculated and added to the initial guess, and we end up with the next trial spectrum,
  $u_1 = u_0 + (\boldsymbol{D} - f_0)$

- This is then repeated according to the following iteration scheme,
  $u_{i+1} = u_i + (\boldsymbol{D} - f_i)$

This method is performed until $f_i \approx \boldsymbol{D}$ within the experimental uncertainties [3]. It is important to note that for each new iteration, the oscillations between channels increase, as the solution approaches the inverted matrix solution $u = \boldsymbol{R}^{-1}\boldsymbol{D}$, which exhibits large oscillations. [2][3]

2.1 The Compton Subtraction Method

As the resulting spectrum from the folding iteration method often contains some degree of fluctuations, the Compton subtraction method is performed to obtain a significantly more stable spectrum.

The first step is to define a new spectrum $v(i)$ as the observed data excluding the Compton contribution:

$$v(i) = p_f(i)u(i) + w(i), \tag{3.3}$$

where $u(i)$ is the spectrum obtained from the folding iteration method, which multiplied with p_f gives the full energy contribution. The remaining contributions are contained in $w(i) = u_s + u_d + u_a = p_s(i)u(i) + p_d(i)u(i) + \sum p_{511}(i)u(i)$, representing single escape, double escape and annihilation (note the missing Compton contribution "u_c"). To match the observed energy resolution, each contribution is then smoothed with a Gaussian function. Next, we subtract this from the raw spectrum to obtain the Compton background spectrum:

$$c(i) = r(i) - v(i). \tag{3.4}$$

This spectrum may exhibit significant oscillations, and is thus further smoothed. This smoothing carries a low risk of loss of important information due to the nature of the spectrum not containing any sharp, narrow peaks. After this smoothing procedure on the individual contributions, we now "return" to the unfolded spectrum like so:

$$u(i) = \frac{r(i) - c(i) - w(i)}{p_f}. \tag{3.5}$$

Finally, to get closer to the true number of events, we correct for the total detector efficiency:

$$U(i) = \frac{u(i)}{\epsilon_{tot}(i)}. \tag{3.6}$$

This final spectrum shows higher stability compared to the result of the iteration method, while keeping similar statistical fluctuations to the raw spectrum. [3]

3   Fully Bayesian Unfolding

Bayes' theorem succinctly describes what we are asking for in the problem of unfolding, showing the relation between the truth spectrum $\boldsymbol{T}$, and the data we have obtained $\boldsymbol{D}$.

$$P(\boldsymbol{T}|\boldsymbol{D}) \propto L(\boldsymbol{D}|\boldsymbol{T}) \cdot P(\boldsymbol{T}) \tag{3.7}$$

The expected truth spectrum T and the raw spectrum D are binned with N_t and N_r bins, respectively. Each bin in T is assigned a prior probability distribution, describing our belief of the number of events expected to be present. We assume the data follows a Poisson distribution, meaning

$$L(\boldsymbol{D}|\boldsymbol{T}) = \prod_{r=1}^{N_r} \frac{f_r^{D_r}}{D_r!} e^{-f_r} \tag{3.8}$$

where

$$f_r = \sum_{t=1}^{N_t} T_t \cdot R_{tr}. \tag{3.9}$$

Here, R_{tr} is the element of the response matrix $R_{N_t \times N_r}$, corresponding to the probability that an event produced in the truth bin t is observed in the reconstructed bin r: $P(r|t)$. If we wish to include the background spectrum, all we have to do is add it to the sum:

$$f_r = \boldsymbol{B}_r + \sum_{t=1}^{N_t} T_t \cdot R_{tr}. \tag{3.10}$$

The next step is to employ a sampling scheme of the parameter space, usually a MCMC algorithm, to calculate $L(\boldsymbol{D}|\boldsymbol{T}) \cdot P(\boldsymbol{T})$ and arrive at a posterior distribution per bin in the expected truth spectrum.

3.1 Priors

- Explain prior dist for each bin

As mentioned above, each bin in the spectrum is assigned a prior distribution. This means we are choosing the exact range and weighting of values we believe to be possible for that bin, independent of other bins. In fact, since the prior has to equal 0 outside its defined range, we say that it is impossible for there to be values beyond the boundaries. Since we are dealing with physical experiments, these boundaries need to be finite, and thus we are forced to restrict the realm of possibilities to whatever deem reasonable.

- Uniform

There is practically an infinite amount of choices one can make for assigning a prior, depending on what knowledge one has beforehand. If one wishes to make the least amount of assumptions about the truth, a *uniform* prior is suitable. The pdf of the uniform distribution is given as:

$$f(x; a, b) = \begin{cases} \frac{1}{b-a} & \text{for } a \leq x \leq b \\ 0 & \text{otherwise} \end{cases} \tag{3.11}$$

Ref? This flat distribution assigns equal probability to every outcome in the space of possibilities. The only assumption to be made here is determining the boundaries on this space. Complete ignorance would strictly be represented with a uniform prior without

any boundaries. This would mean we believe all numbers on the interval $[-\infty, \infty]$ to be equally likely in a one-dimensional space. Such a space is of course not possible to explore completely, and otherwise extremely large limits will be computationally unfeasible. This is especially true considering the fact that many problems are complex and demand multidimensional parameter spaces. In addition to this, unfolding in physics is often related to physical experiments pertaining to the counting of a number of events measured by a detector. In these cases, the existence of negative counts is unphysical, meaning a lower prior limit can safely be set to 0 (Discuss possibility for negative counts?).

Choosing the upper limit is not as straightforward. The ideal choice would be the largest possible limit that still allows for reasonable computational performance. Of course, if we have some knowledge about the size and location of the domain of the possible truth-values, there is no need to pick a limit located significantly beyond this domain. Computational resources are wasted if spent on exploring a region we strongly believe (know?) will not improve our estimate. A good check is to fold the upper prior limit with the response and make sure the raw data is contained within.

Make sure the folded of prior contains the raw spectrum?

In this thesis, an upper prior limit of 10 times the raw data will be used for the uniform prior. In other words, we believe that the true value must be contained within an area relatively close to the observed value.

- Image of uniform distribution

- Logarithmic (using 'interpolate' in pymc3)

Another prior distribution we will use is the *log-uniform* distribution, also called the reciprocal distribution ref?. This distribution has the characteristic that its logarithm is uniformly distributed. What this means for our prior belief is that each order of magnitude is given equal probability. In the case of a logarithm with base 10, we say that it is equally probable for our value of interest to lie between limits $a = 10^0$ and $b = 10^1$, as between $a = 10^6$ and $b = 10^7$, even though the second range is much larger. The pdf of the log-uniform distribution is defined as:

$$f(x; a, b) = \frac{1}{x \ln(b/a)} \quad \text{for } a \leq x \leq b \text{ and } a > 0. \tag{3.12}$$

Ref?

- Image of logarithmic distribution

Using the log-uniform distribution allows us to define a very large range of possible truth-values while keeping a high probability for values close to 0. The amount of counts per experiment is finite, and in cases with significant differences between peaks and valleys, we do not want to 'dampen' these by probabilistic distribution of counts into bins which should be containing none.

Say we know there exists one or multiple peaks in our truth-spectrum consisting of a very large amount of counts, i.e. $\sim 10^{10}$. If we also know that other bins in the spectrum should have close to 0 counts, how do we make sure both of these conditions are met? If we were to use a uniform prior between 0 and 10^{10}, we would firstly have an incredibly large space to explore, with 10^{10} possible values for each bin in the spectrum. Secondly, the probability of sampling a value close to 0 would be very small. Let's say that any value between 0 and 10000 is considered 'close' to 0, which itself seems very imprecise. According to the uniform prior, the probability of the true value being 'close' to 0 is thus:

$$P(0 \leq T_t \leq 10^4) = \int_0^{10^4} \frac{1}{10^{10} - 0} dT_t = \frac{10^4}{10^{10}} = 10^{-6} = 0.0001\%, \tag{3.13}$$

and the same result holds for values equally 'close' to the maximum of 10^{10}. This low probability means we might run out of computational resources long before our algorithm gets to explore those areas.

Now, if we instead use the log-uniform distribution as our prior, the probability of a value close to 0 is much higher, while still allowing for those tall peaks.

$$P(1 \leq T_t \leq 10^4) = \int_1^{10^4} \frac{1}{T_t \ln (10^{10}/1)} dT_t = 0.4 = 40\%. \tag{3.14}$$

Note here that we integrate from a count value of 1 instead of 0, as the distribution is undefined at $T_t = 0$. Since the logarithm of this function is uniformly distributed, looking at the exponents will give a good indication of the probability value. In the simple case above, the exponents are 4 and 10, $4/10 = 0.4 = 40\%$. Similarly, we can estimate the probability of the area between 10^6 and 10^{10} to be $(10 - 6)/10 = 0.4 = 40\%$, the same result as in eq. (3.14), even though this range is much larger. The estimation turns out to be correct when we perform the proper calculation:

$$P(10^6 \leq T_t \leq 10^{10}) = \int_{10^6}^{10^{10}} \frac{1}{T_t \ln (10^{10}/1)} dT_t = 0.4 = 40\% \tag{3.15}$$

In summary, when we believe the truth spectrum to exhibit a very large difference between minima and maxima, the log-uniform distribution is a good candidate for the

prior. This way, we increase the chance of reaching the proper relation between peaks and valleys, at the price of lower precision for higher values. The high probability for values close to 0 will also allow for less distribution of counts into bins where there should be almost none, due to the nature of probability. Should the true spectrum instead be composed of peaks with similar magnitudes and smaller differences, a uniform prior may be better suited.

The implementation of the prior distributions is discussed in part III.

3.2 Multiplying response with (total) efficiencies

3.3 Likelihood

- Poisson (already mentioned above)

As mentioned above, the likelihood used in FBU is given by the Poisson distribution, given by eq. (3.8). It is important to note that the likelihood is a function rather than a pdf, meaning it does not necessarily integrate to 1.

When we assign the prior probability for our problem, we do so on a per-bin basis, meaning we end up with a set of N independent distributions, represented by histograms, each describing the probability of possible truth-values for one bin. The same applies to the posterior probability, the only difference being the histograms having different shapes, due to the fact that we have been provided new knowledge from the data. This reshaping stems from the multiplication of the prior with the likelihood. One might then be tempted to construct a 1-dimensional Poisson distribution for a given bin, multiply with the prior and call this product the posterior. This is incorrect due to two reasons:

- Firstly, one must remember that the posterior is only proportional to the product likelihood×prior, meaning it may need normalization to be a proper pdf and integrate to 1.

- Secondly, and most importantly, the likelihood cannot be assigned on a per-bin basis like the prior, as it does not consist of N independent distributions of which we can aggregate.

The likelihood is an N-dimensional function dependent on the total collection of data as well as the entire response matrix. For a given bin, a 1-dimensional Poisson distribution based on that data does not equal the contribution from the actual likelihood in that bin, unless our spectrum consists of only one bin. This also means we have no easy way

of plotting the likelihood, should we wish to compare with the prior and posterior in a model test, unless we restrict the spectrum to contain a maximum of $N = 3$ bins and plot the complete multidimensional function. Most experiments are conducted with many more bins than this, however there is still some value to be had from performing such a visualization. Mainly, this will help us achieve an increased understanding of the process of Fully Bayesian Unfolding, its components, as well as the inner workings of the PyFBU-package. Due to its (lack of documentation? and) several layers of abstraction, both in itself and through PyMC3 and Theano, the PARTS are not immediately apparent. The symbolic variables and objects, while computationally efficient, do not allow for simple printing or plotting during intermediate steps. Understanding why the results appear as they do is therefore not straightforward, but we are able to use what we know about the prior and likelihood. The prior is defined by the user, but the likelihood is not. In fact, there is no simple multiplication of prior and likelihood performed in the source code of PyFBU at all. This is due to the way Bayes' theorem is being implemented. In the analythical formula, eq. (3.7), we see the posterior as a rescaled version of the prior, through multiplication with the likelihood. In the code, there is instead of this product, a definition of the space for which a sampling algorithm explores. By PyMC3 convention, this space is defined as the likelihood evaluated on the prior, i.e. plugging the prior-values in for T_t in eq. (3.9). This is shown by creating an object of class 'Poisson' from the PyMC3 package, with the prior (folded with the response) and data as arguments. The class refers to one of the built-in distribution classes found in PyMC3. To make sure we are correct about this indeed representing the likelihood, we will want to compare the resulting posterior with a Poisson distribution we construct ourselves, multiplied with the prior. If the posterior has the same shape and location as this product, we have verified our knowledge of the likelihood and its parameters. As mentioned above, we will have to plot the entire multidimensional Poisson distribution to show a correct picture. Therefore, a 2-bin constructed spectrum will be used for this purpose. This implementation will be discussed in part III.

Show image of 2d likelihood vs posterior? Or do this in the results section? Either way, mention that since the prior is uniform, the likelihood alone will have the same shape and location as likelihood*prior

- Modified Poisson to take into account the total amount of counts

With a greater understanding of what happens under the hood, we can experiment with modification of the likelihood. We believe the Poisson distribution to be a good represen-

tation of the data, and will not switch it out completely. Such a switch is possible through PyFBU and PyMC3, but we will only perform a modification of the standard Poisson.

3.4 Sampling

- NUTS

There are several sampling methods possible for the problem of unfolding, a common example being Markov Chain Monte Carlo (MCMC) algorithms such as the Metropolis-Hastings algorithm. In the PyFBU-package, a variant of a Hamiltonian Monte Carlo (HMC) Markov Chain Monte Carlo algorithm is the default sampler. HMC aims to be much more efficient than regular MCMC algorithms by avoiding both sensitivity to correlated parameters and random walk tendencies [4]. A drawback to this is a significant sensitivity to step size as well as the number of steps, requiring manual tuning of these parameters. To circumvent this, Hoffman and Gelman created the No U-turn Sampler (NUTS), a variant of HMC which removes having to specify the number of steps. They also implemented an adaptive step size, meaning no manual tuning is necessary for running NUTS. Furthermore, they observed similar to better performance than other fine-tuned HMC algorithms [4]. The NUTS algorithm is implemented in the PyMC3 package [5] and is the default sampling algorithm in PyFBU.

- Initializing?

PyMC3 has several methods for initializing NUTS, the default being 'jitter+adapt_diag' CONTINUE Another sampling method which will be used in this thesis is called Automatic Differentiation Variational Inference (ADVI) [6].

It is included in PyMC3 as a possible choice for the **initialization** of NUTS. In some cases, the use of this initialization will help when FBU would otherwise crash. Maybe due to the 'jitter' part of 'auto'?

3.5 Posterior inference

Now that the unfolding has been performed, how do we interpret the resulting posterior distribution? While other methods may only return a point value, not necessarily accompanied by the uncertainties, FBU allows us to directly look at the final distribution per bin, and thus observe the result and its corresponding degree of belief. Of course, we are able to quantify these concepts in multiple ways. Here, we take a look at some of the methods of posterior inference.

3.5.1   Point estimates

Since we are dealing with 1-dimensional raw spectra visualized as plots with counts on the y-axis, and energy (bins) on the x-axis, it is desirable to represent the unfolded result the same way. The final output from FBU is a list containing N sets of posterior samples, allowing us to create N histograms representing the respective posterior distribution in each bin. One can then simply stack these histograms to form a band through the entire energy range, where higher probabilities can be shown with higher color intensities. However, it is customary to operate with point values for the unfolded spectrum when performing further analysis, like the results OMpy supplies. Point estimates will also allow us to directly compare performance with the folding iteration method, of which point values are the only output. Finally, error metrics such as the mean squared error (MSE) are evaluated on point values, and allows for a quantitative measure of performance. We can use this to compare the **folded** output with the original raw spectrum, as well as the regular output with the true spectrum, should we possess it.

It is important to remember that a point estimate does not summarize an entire distribution, and may in many cases paint a wrong picture. In these cases, the fact that we can access and look at the complete posterior at any time may be the greatest advantage of using FBU.

Write about aggregating estimates to a final spectrum and compare with raw, compare folded with raw!

We will consider three different point estimates, the posterior mean, median and mode:

- Posterior mean: The mean of the posterior distribution which minimizes the mean squared error (MSE) [7].

- Posterior median: The median of the posterior distribution which minimizes the expected absolute error [7].

- Posterior mode: The mode of the posterior distribution, also called the Maximum A Posteriori (MAP), which represents the most likely value for the parameter in question. This does not take into account any skewness of the posterior nor the existence of multiple modes of similar magnitudes.

3.5.2   Credible intervals

The credible interval is the Bayesian version of the frequentist confidence interval. It depends on the posterior and is defined as any interval that encompasses a certain percent

of the posterior density. The difference between confidence and credible intervals is subtle, but not negligible. In the case of frequentist inference, the parameter in question, lets say θ, is treated as an unknown, but fixed value. The limits of the confidence interval are treated as random variables. Therefore, a confidence level of 95% means that for 100 repeated experiments, 95 of the confidence intervals will contain θ. Note that this does not mean there is a 0.95 probability of finding θ in every confidence interval. [8][9]

For bayesian inference however, the random-trait is switched, with the credible interval limits being fixed, and θ treated as the random variable. The credible interval takes our prior belief into account, while the confidence interval relies only upon the data. A 95% credible interval covers 95% of the posterior and can then be said to contain θ with a probability of 0.95. [8][9]

There are many types of credible intervals, the only requirement being that it covers a certain amount of area of the posterior. Some examples of ways of constructing credible intervals are:

- Using the posterior mean as the interval center.

- Making sure the probability of being outside the interval is equal on all sides (equal tailed).

- Making the interval as narrow as possible, the Highest Posterior Density interval (HPD). This will include the most likely values, as well as the mode of the posterior if it is unimodal.

We will be using the HPD interval which, together with the point estimates mentioned above, will give a solid estimate of the true energies of the γ-ray spectrum.

4   The FBU-package?

5   PyMC3?

- Built-in distributions possible to be used for both likelihoods and priors, such as Uniform, Normal, Poisson etc, as well as Truncated versions of some.

- Custom distribution! 'Interpolated' using x-values and pdf-values.

5.1 Theano?

6 Error statistics? MAE (MSE), R2-score, χ^2 others?

- Compare unfolded with truth (if known)

- Compare unfolded*response with raw

- Residual plots for both

7 1-dimensional test spectrum

8 2-dimensional test spectrum

- Compare posterior with likelihood*prior

9 28 Si spectrum

- Compare result with Valas, using logscale prior, modified likelihood?

- Background?

Valsdóttir found that, when the background was known, including it in the unfolding significantly improved the results.

10 146 Nd spectrum

- 250 channels

- Background, nanoseconds

- 500 channels

- Background? nanoseconds?

- 453 keV

  Discrepancy at lower energies, unavoidable with this response, we have information to correct this. Maybe on the other states too? Results should match OMPy and thats what we want?

- 1-1.4 MeV

- 6-6.2 MeV

11 Model testing

- Cannot construct 1D likelihood Poisson distribution around data in bin X due to cross-bin dependencies.

- 2D example with 2D likelihood plots.

- Prior must be large enough such as the folded prior includes the observed counts.

- Can compare 1D prior and posterior.

- Can compare 2D likelihood and posterior if we only have 2 bins.

11.1 Synthetic data

For easier and more predictable testing, a synthetic data set is used for the raw spectrum. It consists of 3 excited states, a simplified representation of a physical case.
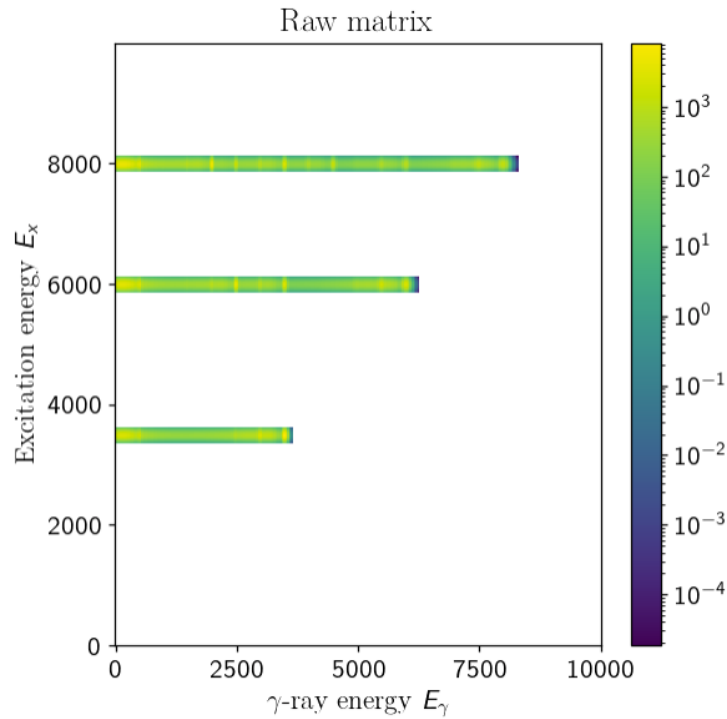
Figure 3.1: Synthetic raw $E_\gamma - E_x$ matrix.

11.2 Bayesian terms

An interesting aspect to look at is the terms in Bayes' theorem after unfolding has been performed. We should be able to reproduce the shape of the resulting posterior samples by multiplying the prior and likelihood. As the likelihood depends on f_r, rather than the truth-values t, direct comparison between this and the other terms is not easy at first glance. To arrive at comparative foundation, we perform the following modifications to the prior and the posterior to achieve f_r-dependence:

$$P(\boldsymbol{T}|\boldsymbol{D})_{f_r} = \boldsymbol{TR}, \tag{3.16}$$

$$P(\boldsymbol{T})_{f_r} = \boldsymbol{SR}, \tag{3.17}$$

where $\boldsymbol{S}$ is a matrix containing random samples between the upper and lower prior limits, with shape corresponding to the output $\boldsymbol{T}$. There is no easy way of extracting the likelihood from the PyFBU package, nor its corresponding f_r-values. However, as we know that it is a Poisson distribution, we are able to define a range of f_r-values determined by the prior and posterior, and use these as input to equation (3.8).

11.3 Response matrices

Here, different trial response matrices are tested for examining the impact on the final result, as well as the convergence of the implemented FBU method. As the response matrix is a vital part of the procedure, significant differences are expected when changes are made. In the end, the experimentally determined response should provide the best unfolded spectrum. It is however interesting to see the effect on the resulting Bayesian terms.

11.3.1   Normalized response from OCL

The following figures are results from running FBU using the response matrix from OCL, with normalization performed on each row.
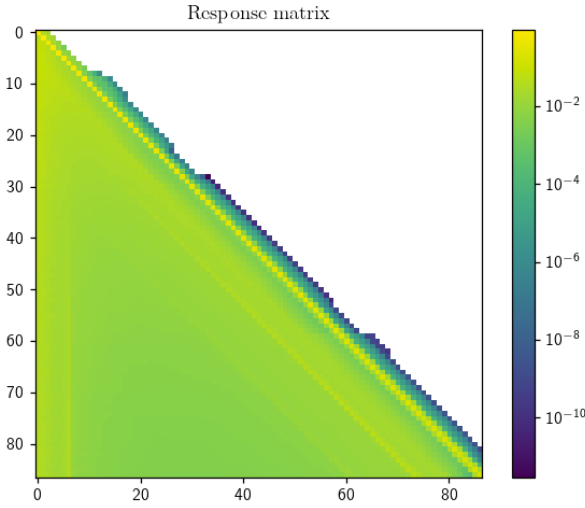
(a) Response matrix
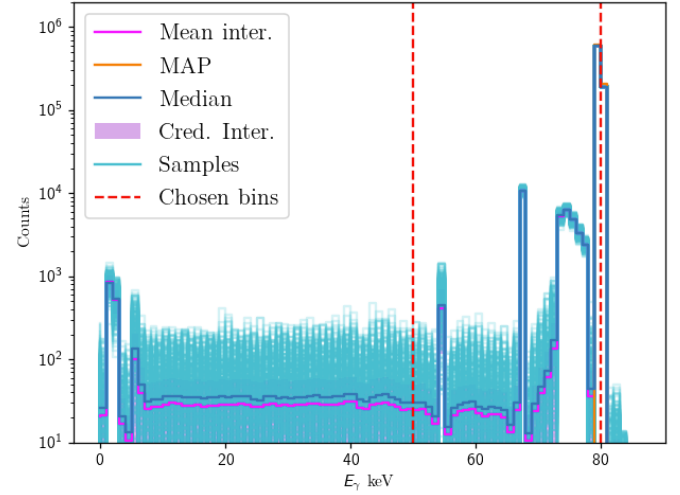
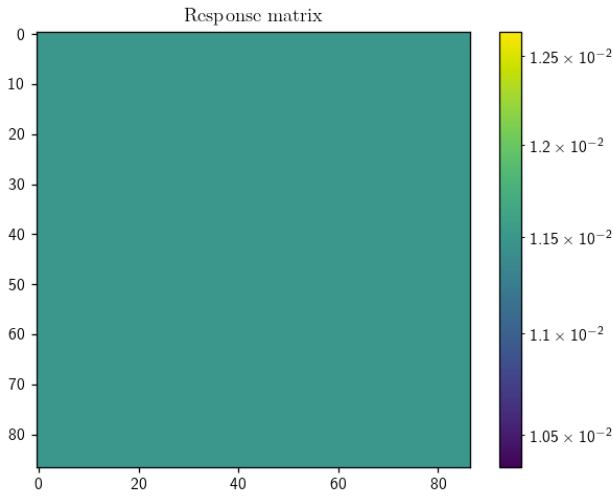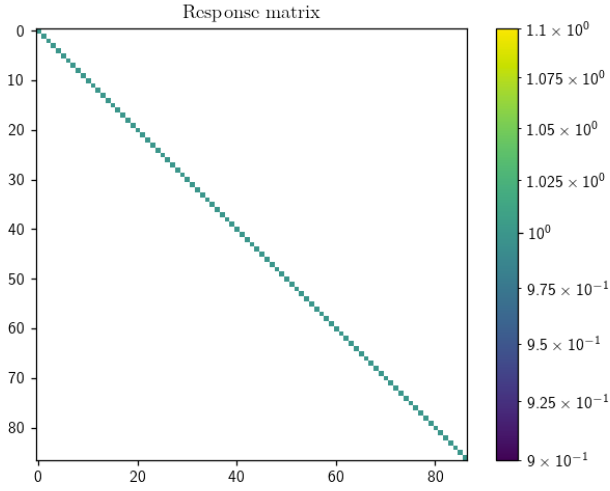(b) Result of unfolding. Dashed lines show the bins chosen for the analysis below.
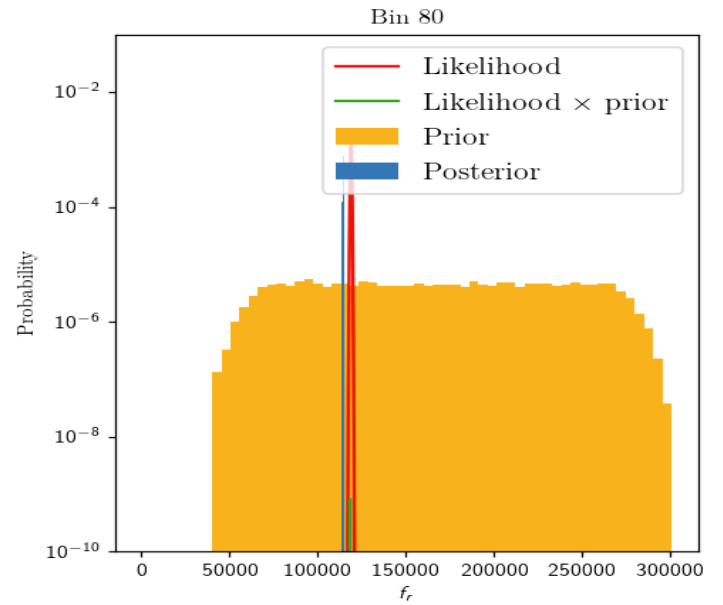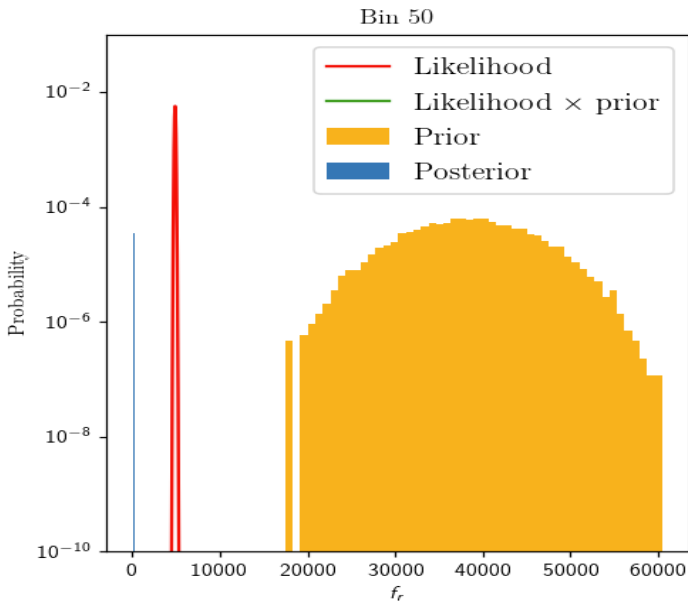
(c) The components of Bayes' theorem after unfolding, for the bins chosen above. Included is also a $L(\boldsymbol{D}|\boldsymbol{T}) \times P(\boldsymbol{T})$-function, which should have the same shape and position as the posterior, only differing by a normalisation constant.

11.3.2   Response from OCL with normalized columns

The following figures are results from running FBU using the response matrix from OCL, with normalization performed on each column instead.
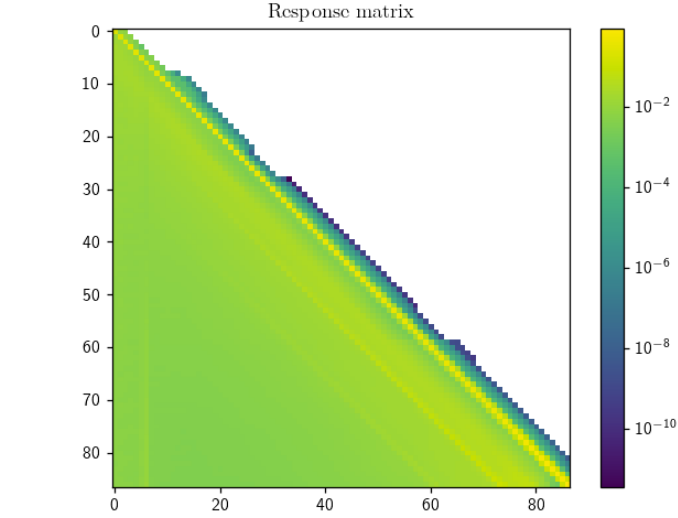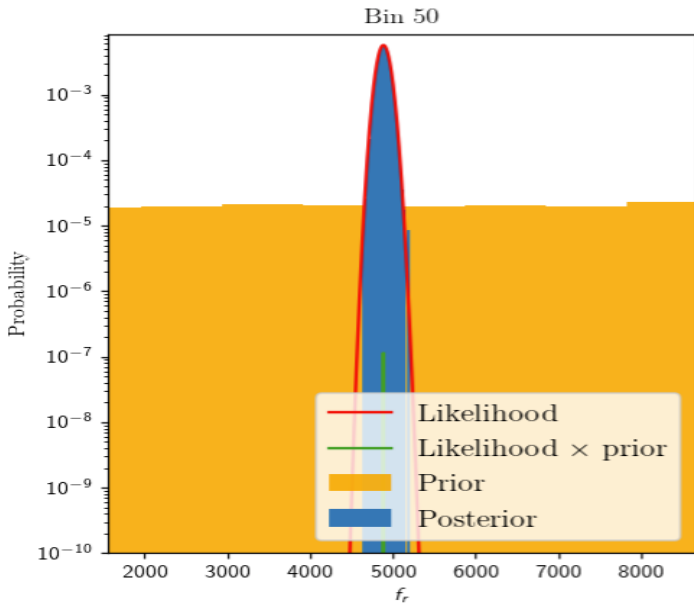

(a) Response matrix
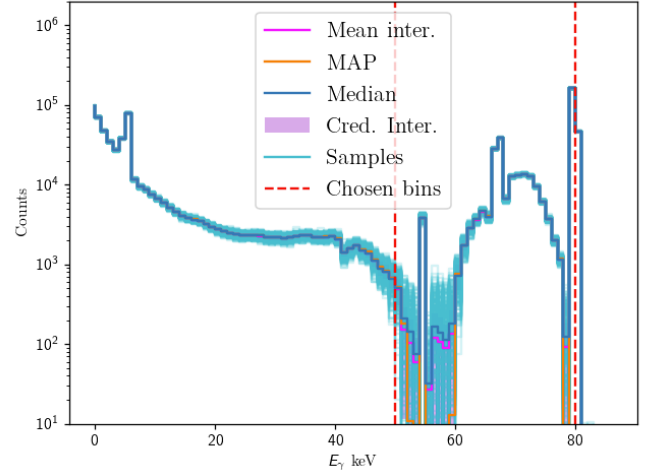
(b) Result of unfolding. Dashed lines show the bins chosen for the analysis below.
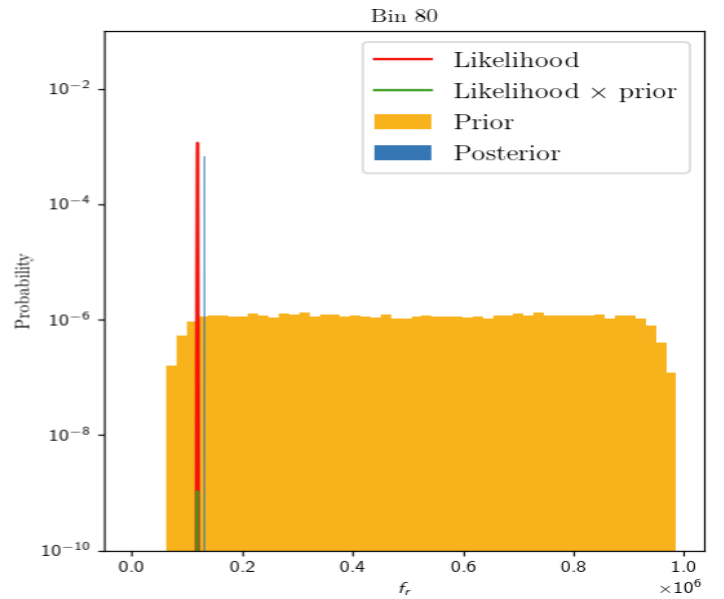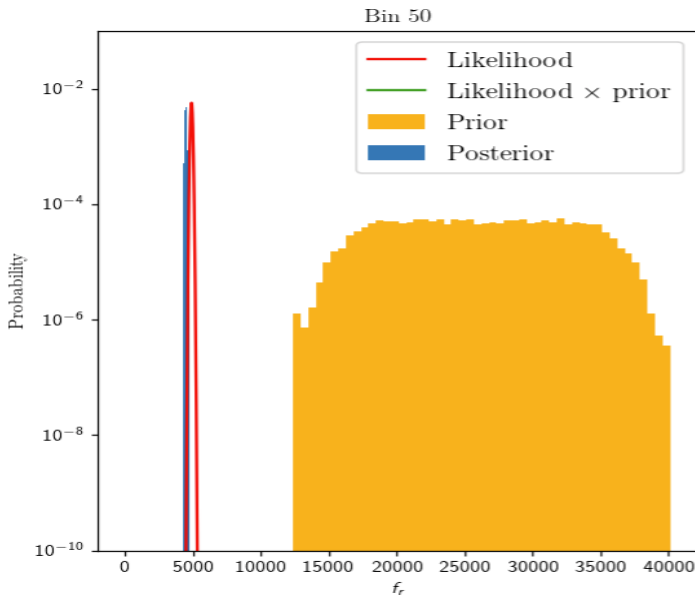
(c) The components of Bayes' theorem after unfolding, for the bins chosen above. Included is also a $L(\boldsymbol{D}|\boldsymbol{T}) \times P(\boldsymbol{T})$-function, which should have the same shape and position as the posterior, only differing by a normalisation constant.

11.3.3   Symmetrized response from OCL

The following is produced using a symmetrized version of the OCL response matrix, that is

$$R = \frac{R_{OCL} + R_{OCL}^T}{2} \tag{3.18}$$
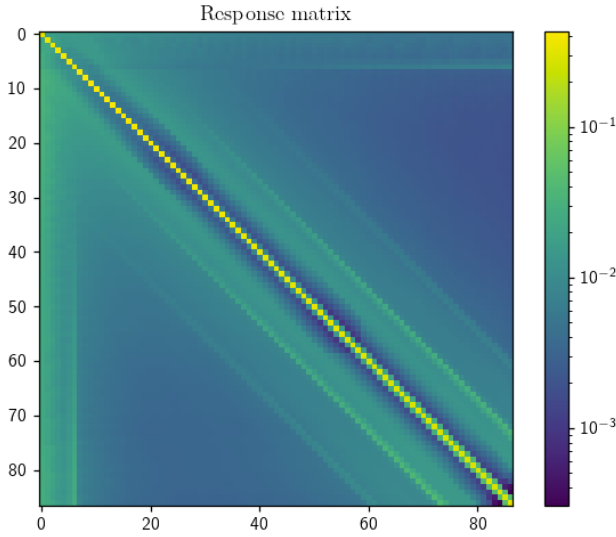
(a) Response matrix
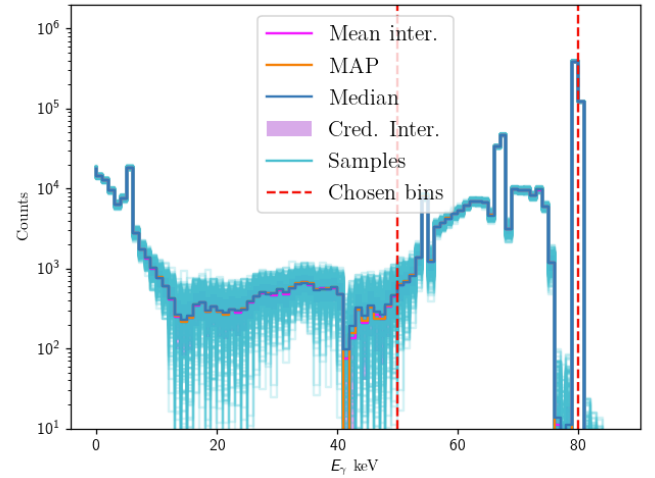
(b) Result of unfolding. Dashed lines show the bins chosen for the analysis below.

(c) The components of Bayes' theorem after unfolding, for the bins chosen above. Included is also a $L(\boldsymbol{D}|\boldsymbol{T}) \times P(\boldsymbol{T})$-function, which should have the same shape and position as the posterior, only differing by a normalisation constant.

31
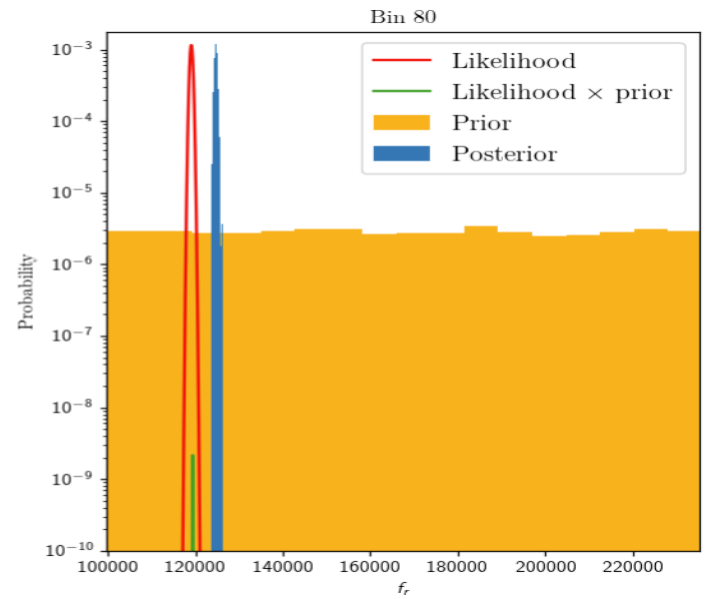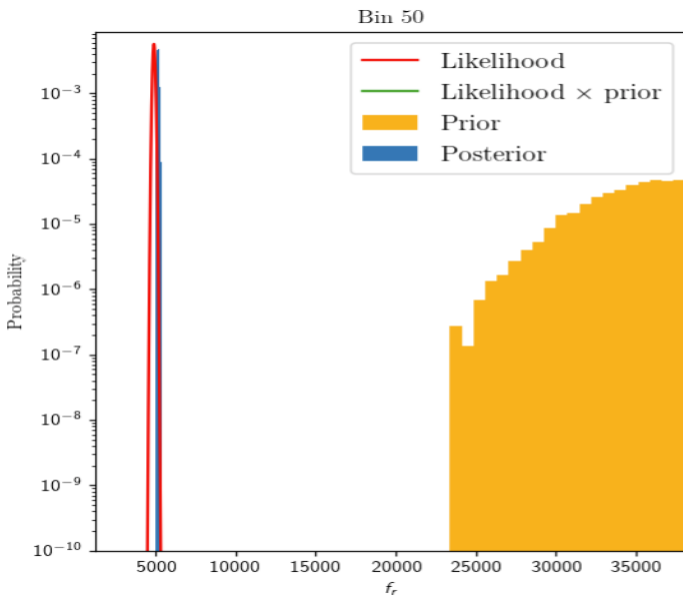
11.3.4   Response as a normalized matrix of ones

Now, the response is a normalized matrix of ones:

$$R^{N \times N} = \begin{bmatrix} 1/N & 1/N & \cdots \\ 1/N & \ddots & \\ \vdots & & \ddots \end{bmatrix} \tag{3.19}$$

(a) Response matrix
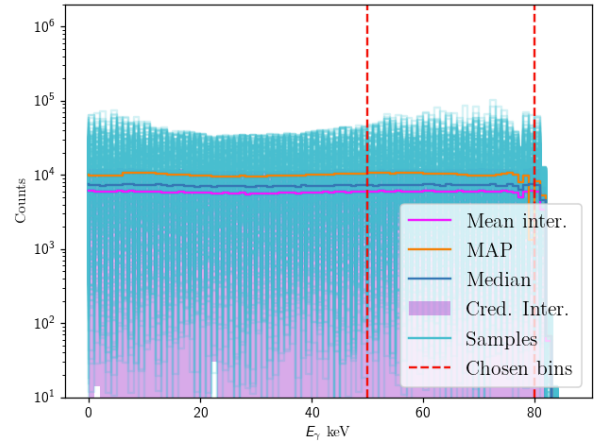
(b) Result of unfolding. Dashed lines show the bins chosen for the analysis below.
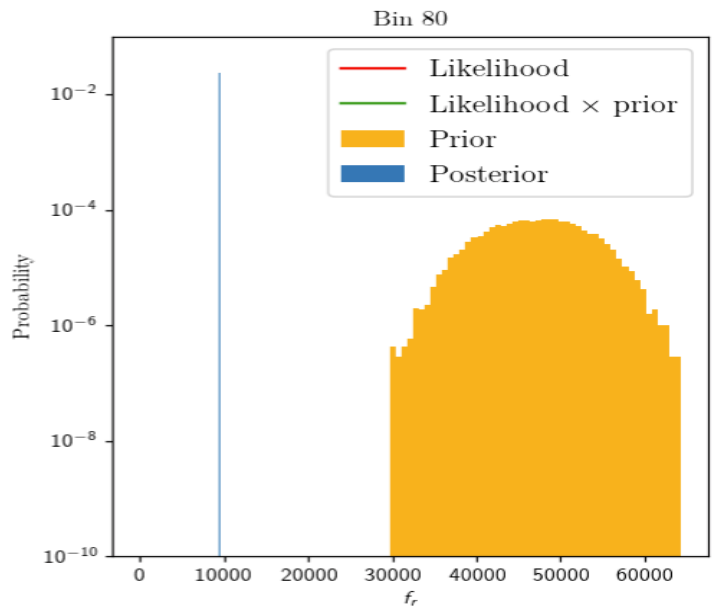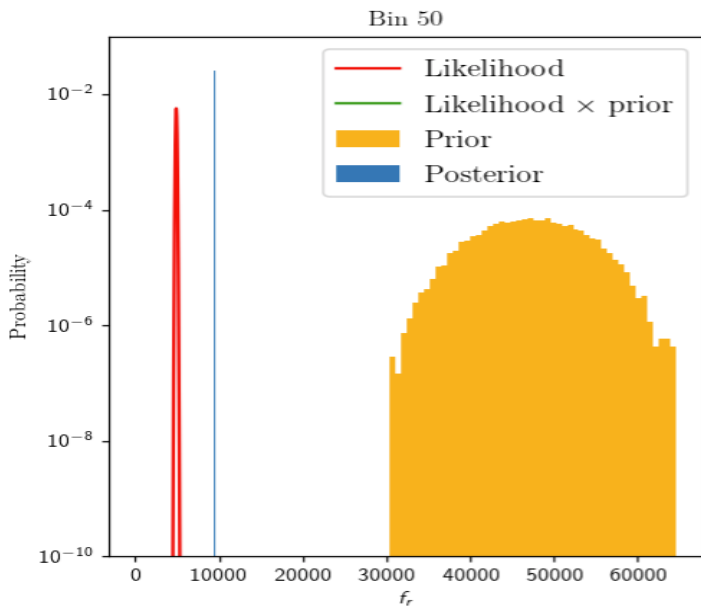
(c) The components of Bayes' theorem after unfolding, for the bins chosen above. Included is also a $L(\boldsymbol{D}|\boldsymbol{T}) \times P(\boldsymbol{T})$-function, which should have the same shape and position as the posterior, only differing by a normalisation constant.

11.3.5 Response as the identity matrix

The results below are produced using an identity response matrix.

$$R = \mathbb{I} \tag{3.20}$$

(a) Response matrix
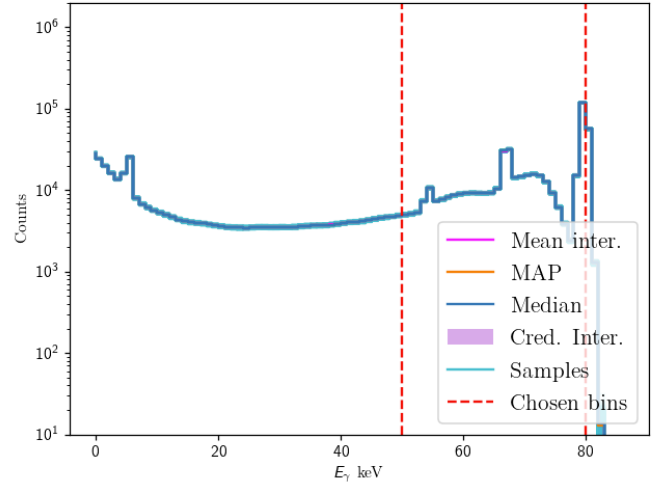
(b) Result of unfolding. Dashed lines show the bins chosen for the analysis below.
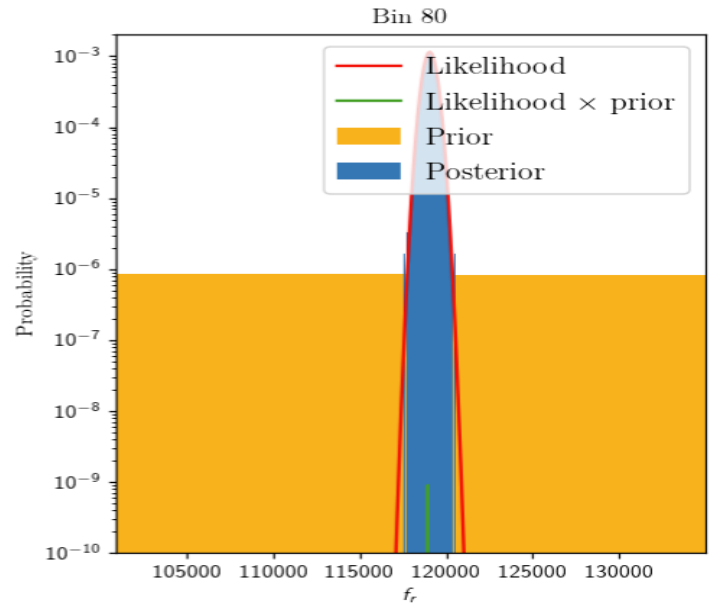
(c) The components of Bayes' theorem after unfolding, for the bins chosen above. Included is also a $L(\boldsymbol{D}|\boldsymbol{T}) \times P(\boldsymbol{T})$-function, which should have the same shape and position as the posterior, only differing by a normalisation constant.

Reproduction

1 Reproduction of results

Under follows a reproduction of the results achieved by Valsdóttir [10]. This procedure allows us to validate the results, as well as providing a benchmark for the new and hopefully improved evolution of these algorithms.

The figures presented as reproductions are outputs of the publicly available Jupyter notebooks on Valsdóttirs GitHub repository [11]. Some discrepancies are seen, pointing to the possibility that the results in Valsdóttirs thesis may stem from newer, locally stored versions of the files that have been made accessible on the repository. This may also be the reason to why the code for some results in the thesis is not found on the repository at all. Therefore, the below sections contain only the results for which corresponding output was found to be produced in the mentioned Jupyter notebooks.

(a) Valsdóttir

(b) Reproduction

Figure 4.1

(a) Valsdóttir

(b) Reproduction
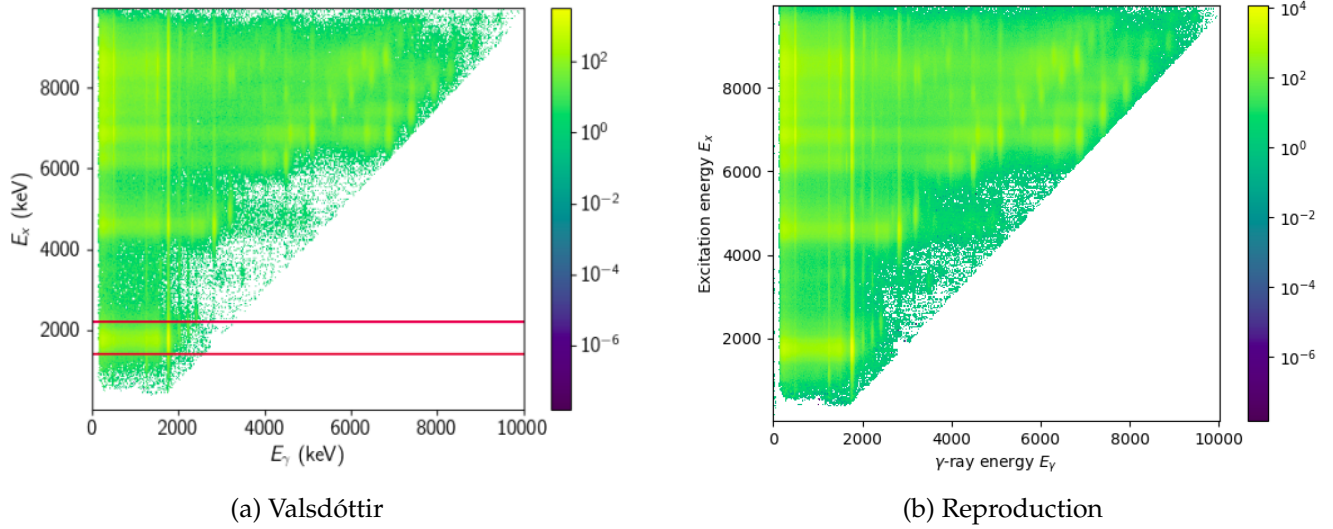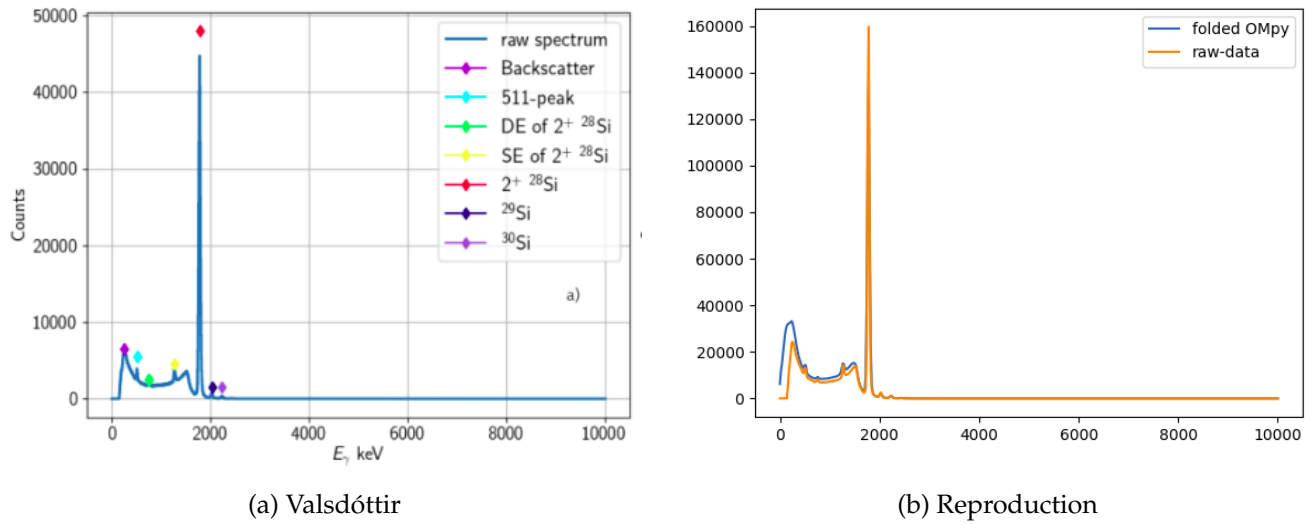
Figure 4.2

1.1 Fully Bayesian Unfolding Spectrum From the First Excited state of ^{28}Si
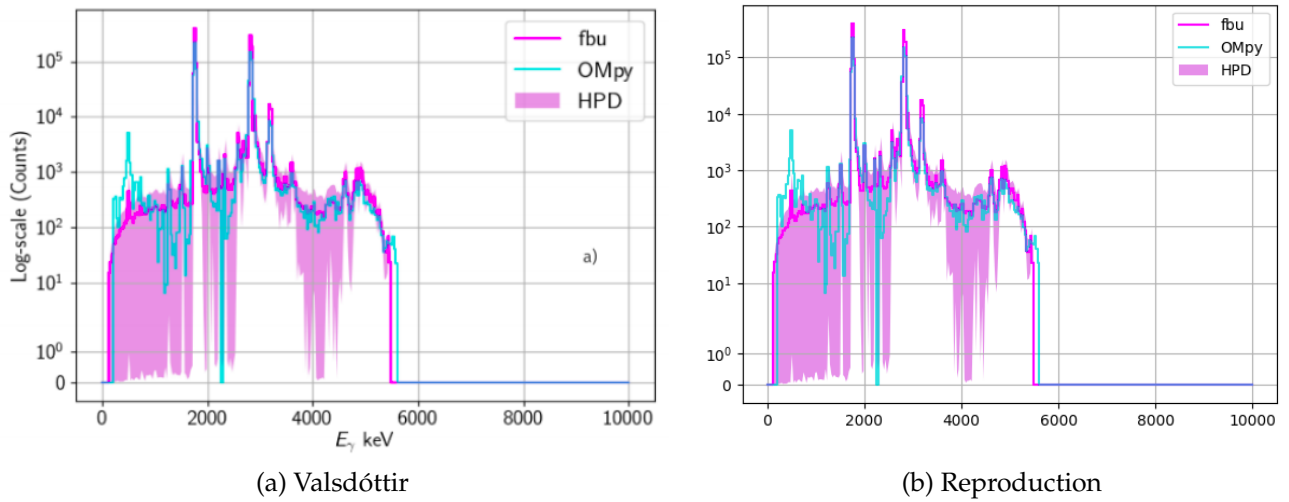
0

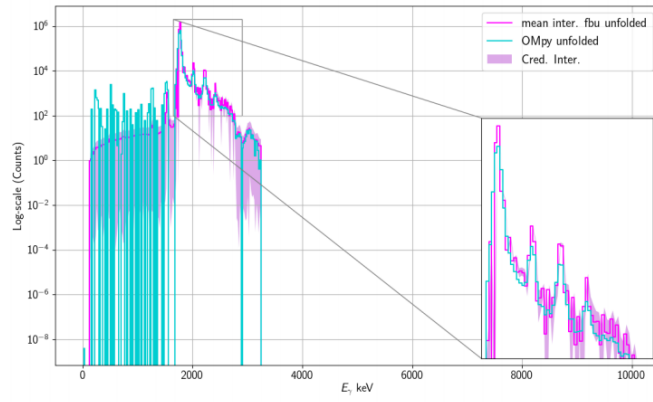(a) Valsdóttir   (b) Reproduction
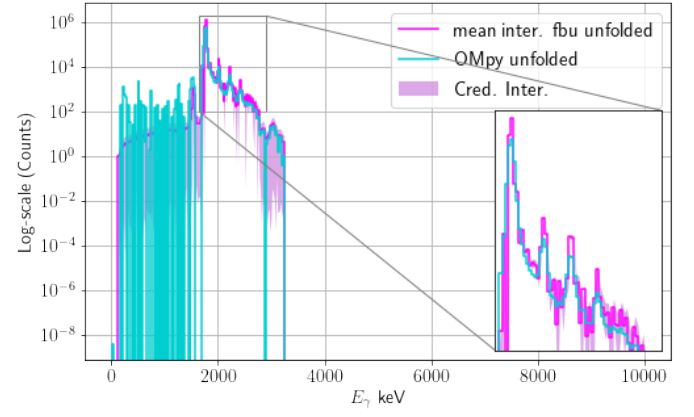
Figure 4.3

(a) Valsdóttir   (b) Reproduction

Figure 4.5

(a) Valsdóttir   (b) Reproduction

Figure 4.6

(a) Valsdóttir   (b) Reproduction
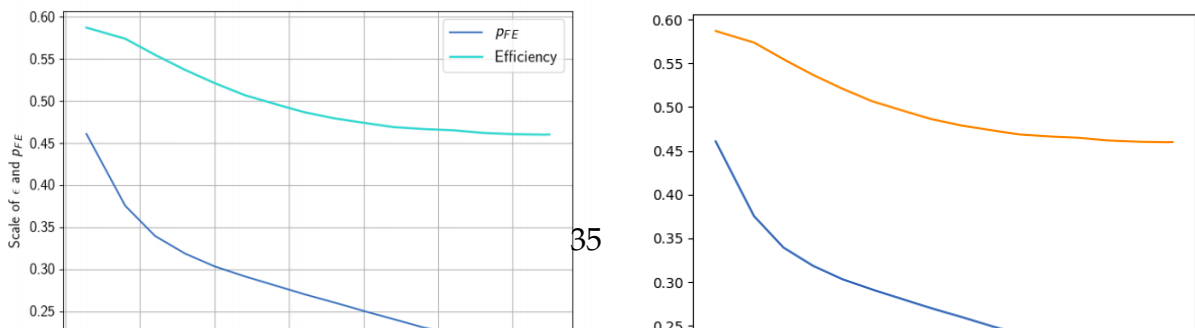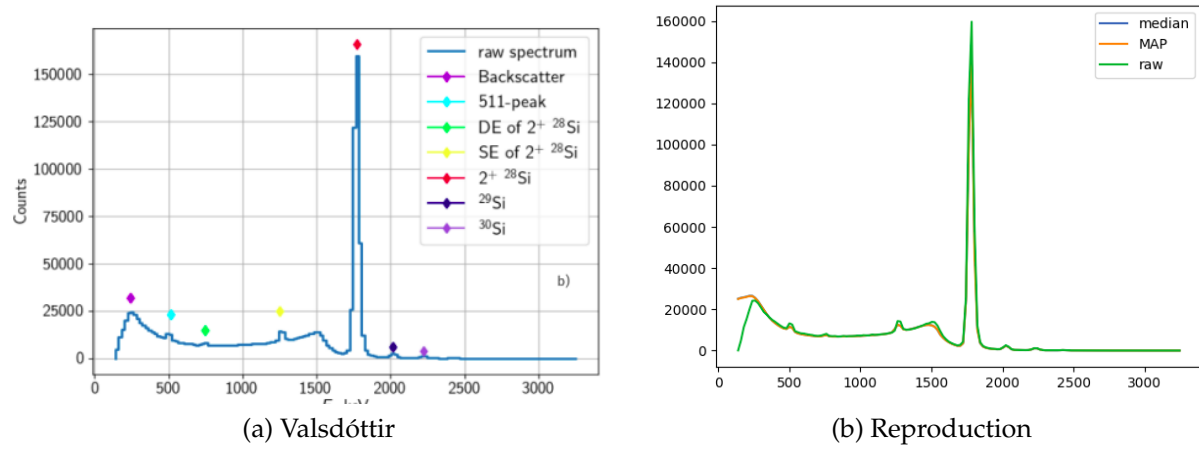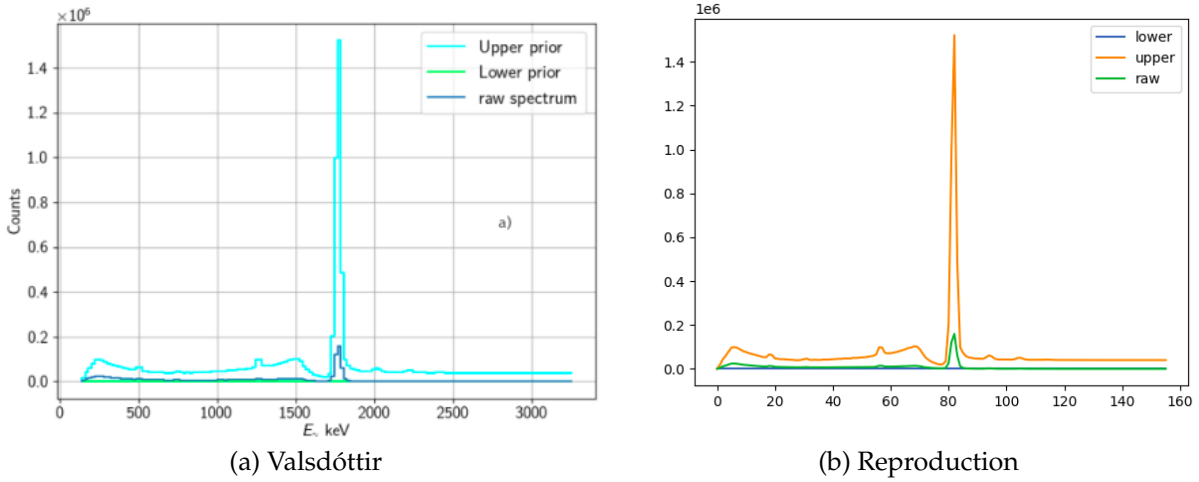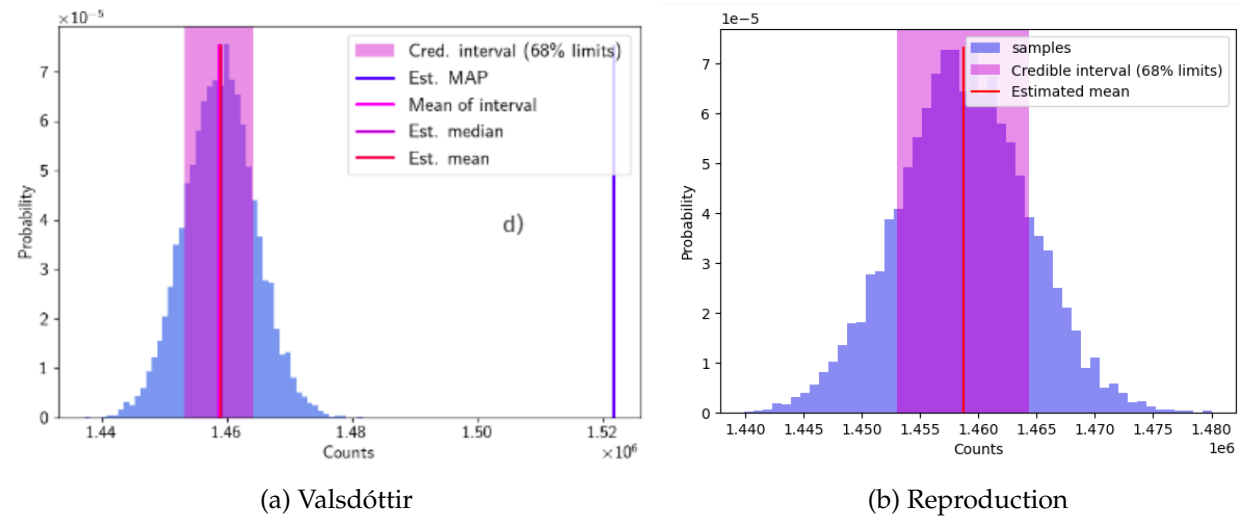
Figure 4.7

1.2 Fully Bayesian Unfolding on first excited state of ^{28}Si including background

(a) Valsdóttir   (b) Reproduction

Figure 4.8

(a) Valsdóttir   (b) Reproduction
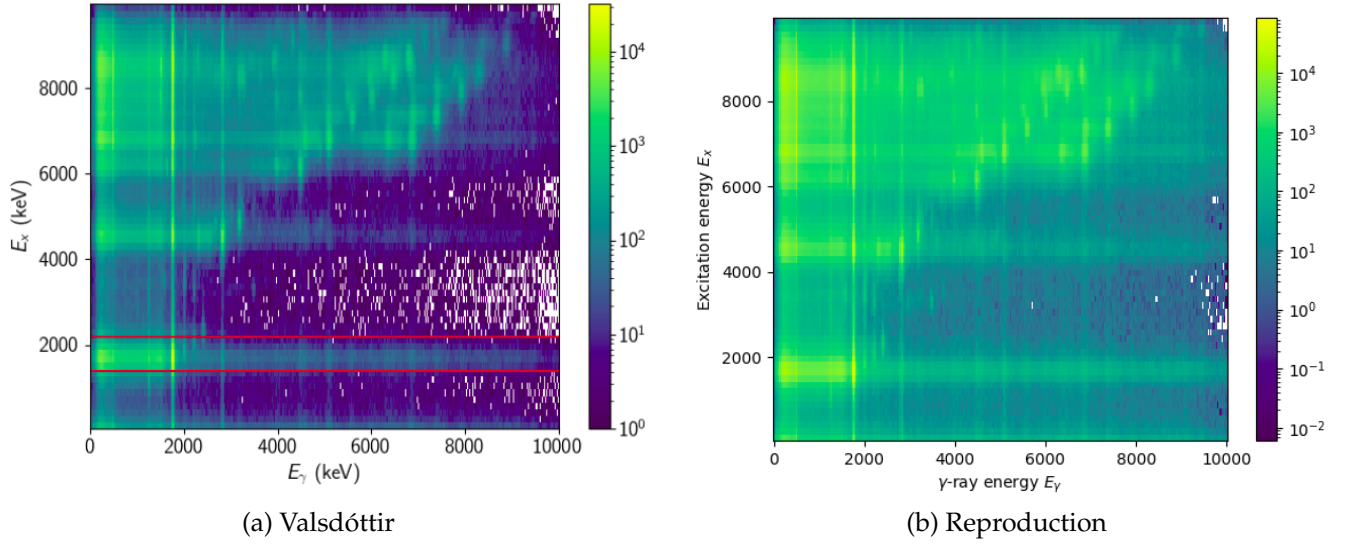
Figure 4.9
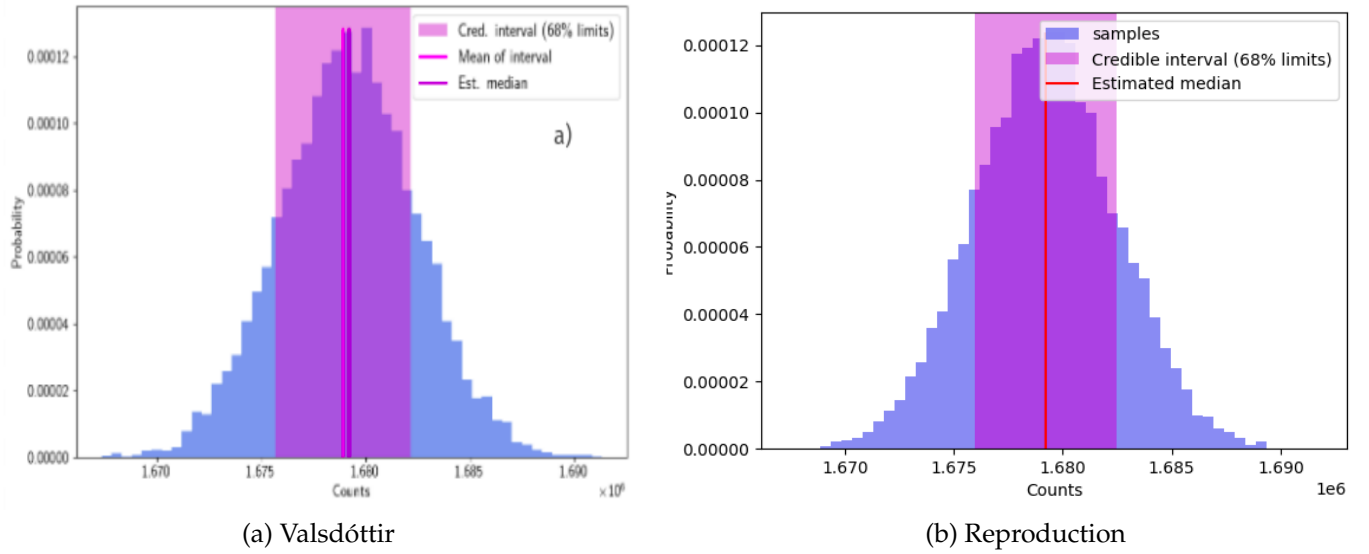
(a) Valsdóttir   (b) Reproduction
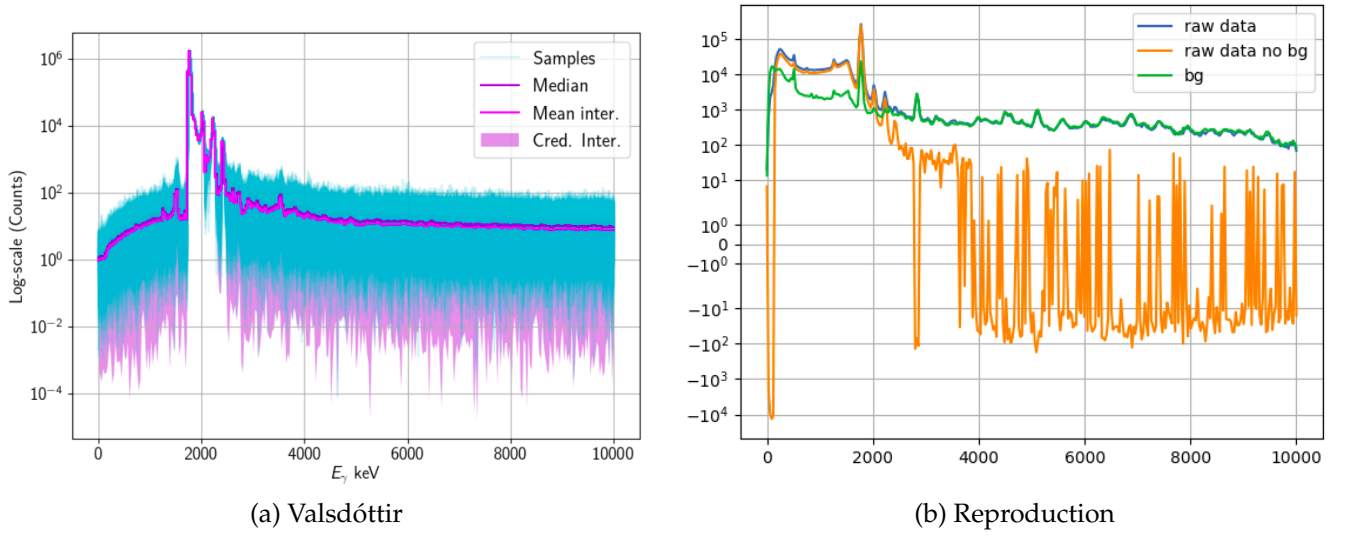
Figure 4.10

1.3 Fully Bayesian Unfolding for all Excited States

(a) Valsdóttir   (b) Reproduction

Figure 4.11

(a) Valsdóttir   (b) Reproduction
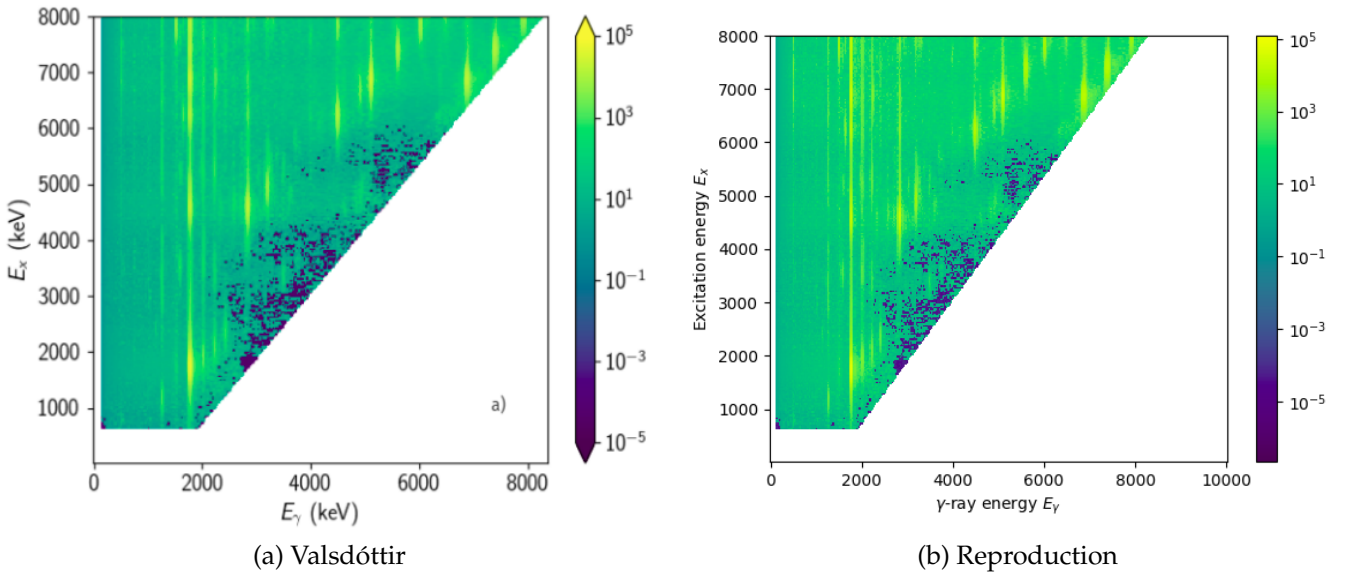
Figure 4.12
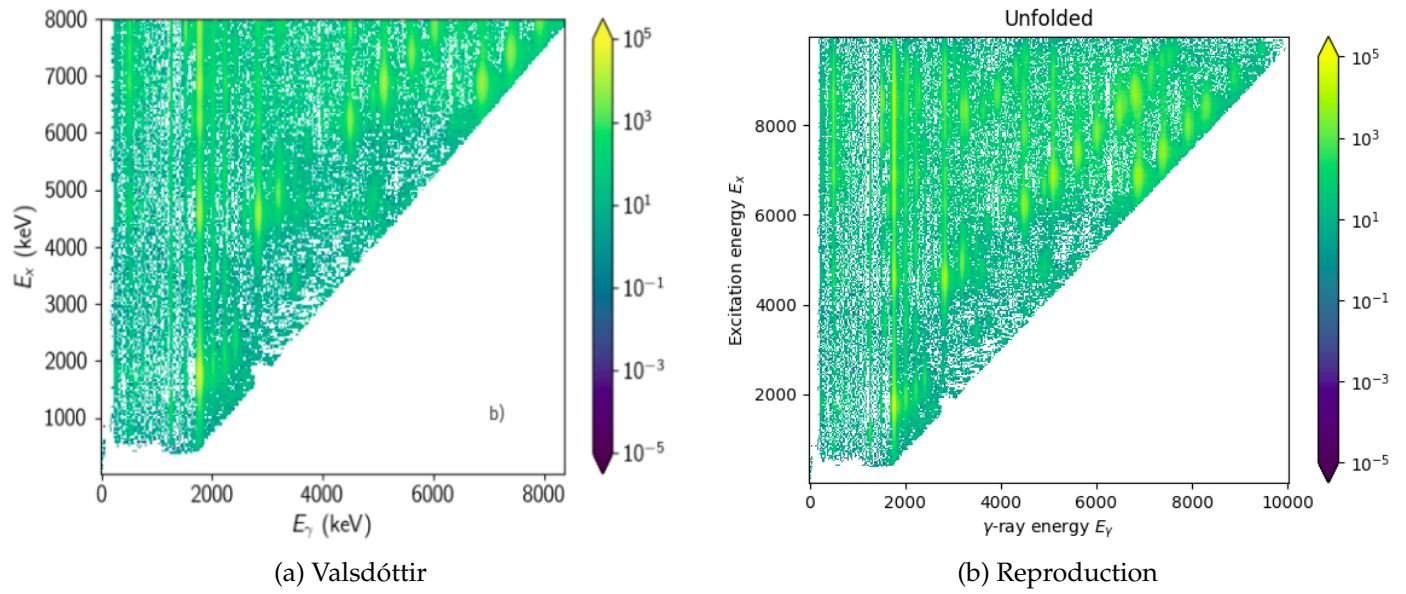
(a) Valsdóttir   (b) Reproduction

Figure 4.13

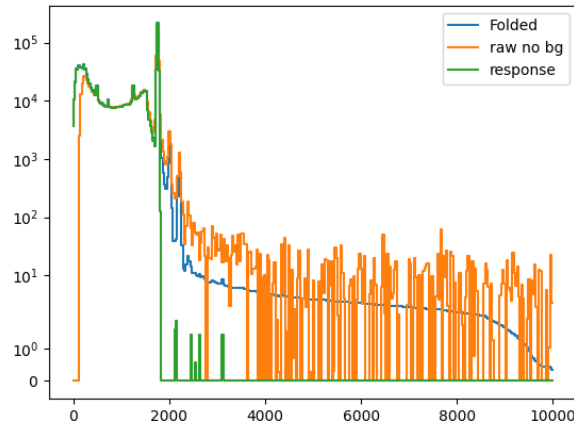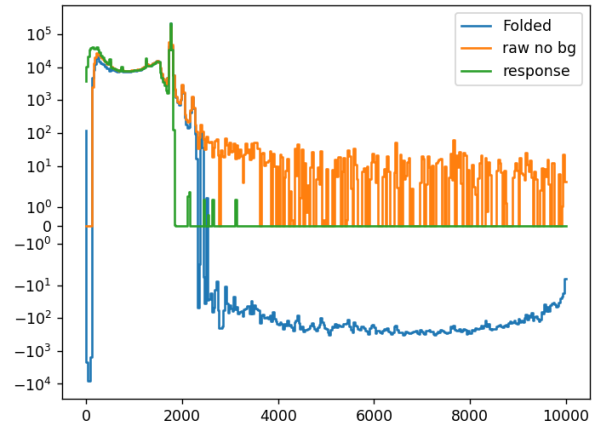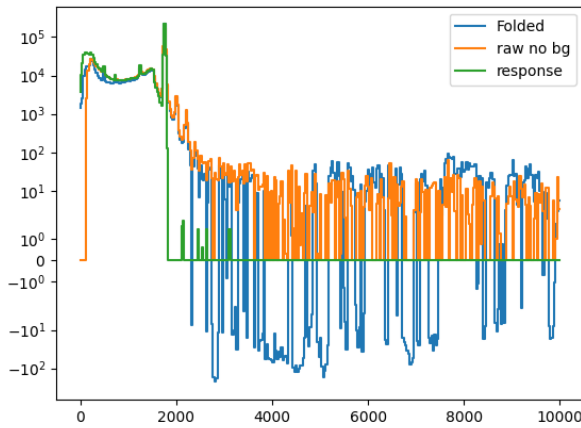(a) Valsdóttir   (b) Reproduction
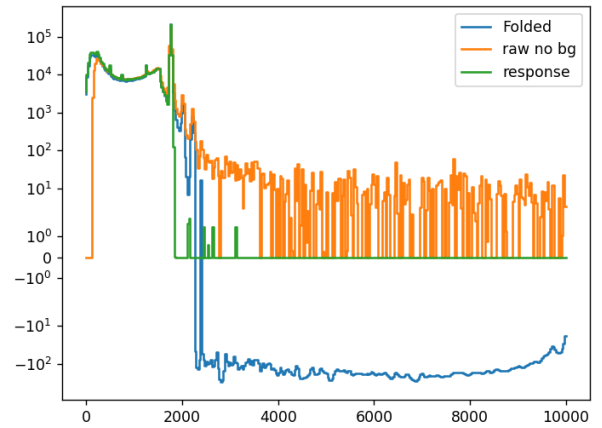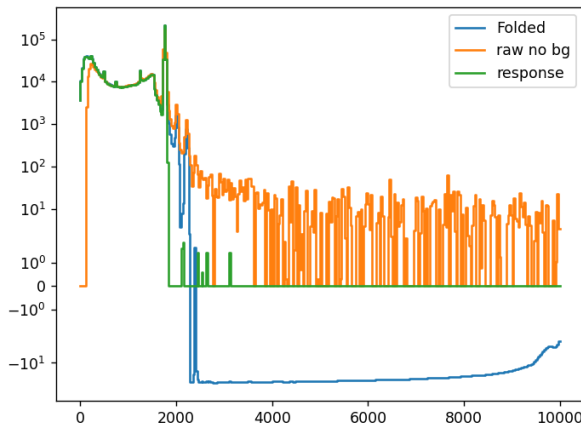
Figure 4.14

(a) Prior lower bound = raw/10
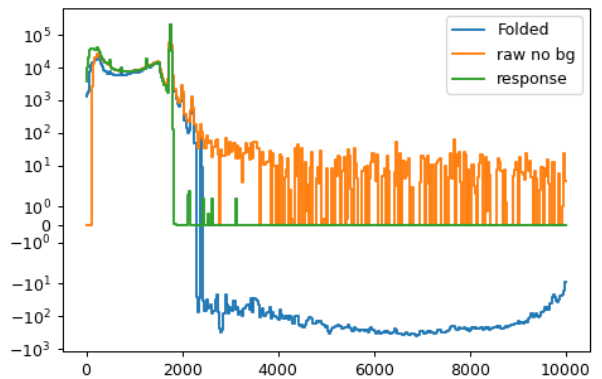

(b) Prior lower bound = raw/50

(c) Prior lower bound = raw/100

(d) Prior lower bound = raw/1000

(e) Prior lower bound = raw−100

(f) Prior lower bound = raw−20000

Figure 4.15

Part III

Implementation

Modification of PyFBU and PyMC3

A significant effort has been made attempting to fully understand the packages used in this thesis. Externally, they are moderately simple to learn and the experience of using them is quite pleasant, should you be content with the limits they pose and the results you receive. Due to the multiple layers of class-references and abstraction, it is not immediately apparent how the code relates to the analytical procedure of FBU, and hence, why the results look as they do. Now, the authors may never have intended for the direct manipulation of their source code, and to expect them to facilitate the possibility would be unfair, seeing as the likely intended use is completely functioning. However, we are in a search of a greater understanding of the process and the results. If we should receive a result we do not expect, we want to know how it came to be, and the ability to fine-tune the individual elements in the name of improvement. This chapter focuses on how PyFBU and PyMC3 is modified to achieve an increased versatility of the unfolding process, by enabling more direct control over the individual Bayesian terms.

The following sections are based on the source code of the PyFBU and PyMC3 packages, as well as the documentation available for PyMC3 [12] [5]. cite the packages somewhere else in this chapter?

1   PyFBU and PyMC3

We start by describing the general setup of PyFBU and how PyMC3 comes into play with the unfolding process. In practice, PyFBU can be said to be used in the following way:

- Create an object of the PyFBU class

- Supply the necessary variables, i.e. observed data, response matrix and the upper and lower prior limits

- Optionally supply parameters such as background data, systematic uncertainties, number of sampling chains and steps, etc.

- Run unfolding

An important part of the process is how the prior is defined. Notice that we only have to supply the limits for the prior, not the distribution itself. This is due to the fact that the uniform distribution is the default prior in PyFBU, and we have some ability to change that by supplying a string with the name of a different distribution. This string is then used to collect one of the built-in distribution classes in PyMC3. There is a good variety of these classes representing many popular distributions used in statistics. Unfortunately, there are only four of these that accept the lower and upper limits as parameters, namely the classes `Uniform`, `DiscreteUniform` (default), `Triangular` and `TruncatedNormal`. If we are to attempt to input the name of any other distribution, we will be met by errors due to the `lower` and `upper` parameters. PyMC3 does however include a class `Bound` that takes the limit parameters and constrains any of the built-in distributions. The resulting distribution is not normalized anymore, and we are still restricted to using the distributions included in PyMC3, unfortunately ruling out the log-uniform distribution (part II, subsection 3.1). Another possibility is the `DensityDist` class, made for supporting custom distributions. This requires supplying a method returning the log-probability of the distribution you want to use, as well as a `random` method if the distribution is to be sampled from. These methods are not straightforward to implement, and attempts to use this class have not been successful by the author of this thesis. Talk about implementation here

When the `run()` method is called, a PyMC3 model is created, wherein the main math and sampling is performed. The prior distribution is created here, using a wrapper-function which returns a PyMC3 object representing a stack of tensors. The important part is found

- Very few dists have lower,upper keywords

- PyMC3 does not have all distributions

- Interpolated allows for complete control, can define the dist outside

- Interpolated allows us to not create an entire subclass of our own. But that might be something to consider, however that necessitates deeper modification of pymc3 than just pyfbu.

- Class diagram

2   Prior choice

- Modificated likelihood

Part IV

Results & Discussion

Synthetic spectra

- 1dim test

- 2dim test (likelihood*prior)

Here, we perform unfolding on a raw spectrum consisting of 2 bins, to display all Bayesian terms and their relation. Even though experimental spectra usually consist of a much larger amount of 100 bins, we have chosen 2 to be able to show the likelihood properly. As mentioned in part II, the likelihood is an N-dimensional function which is not easily decomposed into 1-dimensional contributions. Using 2 bins allows us to plot the likelihood in its entirety on the plane and compare with the posterior. We choose a simple true spectrum $T = (120, 120)$ and construct a 2×2 response matrix with arbitrary values and normalized rows (preferably not the identity matrix, as no changes would happen when folding, i.e. a perfect detector):

$$R_{2 \times 2} = \begin{bmatrix} 1 & 0 \\ 0.5 & 0.5 \end{bmatrix} \tag{6.1}$$

The response matrix is visualized in figure 6.1.

Next, we generate an 'observed' spectrum by folding the true spectrum with the response: Maybe explain why its TR instead of RT

$$D = TR = \begin{bmatrix} 120 & 120 \end{bmatrix} \begin{bmatrix} 1 & 0 \\ 0.5 & 0.5 \end{bmatrix} = \begin{bmatrix} 180 \\ 60 \end{bmatrix} \tag{6.2}$$

Note that by generating the data this way, we take away the inherent randomness of the response matrix. Since it consists of probabilities of an event being reconstructed in bin r given that it originated in truth-bin t, the data would not remain constant for repeat experiments; flipping 10 fair coins does not result in 5 tails and 5 heads every time. A more
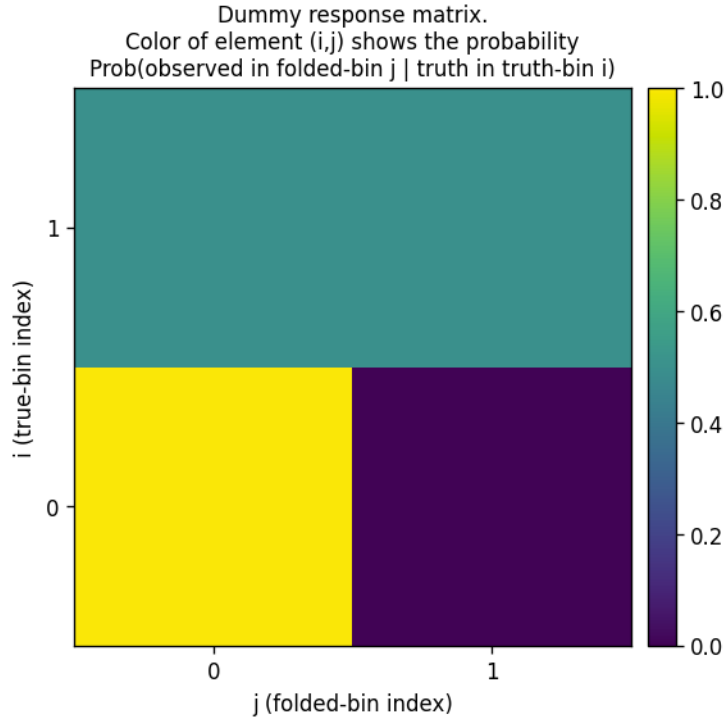
Figure 6.1: The constructed 2-bin response matrix. Note that when plotting, the origin for the indices is at the bottom left corner, as opposed to a mathematical matrix which has indices starting at the top left.

realistic generation of observed data can be performed by randomly sampling a value in each bin according to the given probabilities. mention multinomial distribution? The mean value of these samples will be the same as the result we get from direct multiplication with the response. That is sufficient in this case, where the focus is on investigating the Bayesian terms and verifying our knowledge of the likelihood. Is this true? Should I sample the values instead of direct multiplication? For both bins, we assign a uniform prior in the range $[0, 200]$ since we know the true values, and perform the unfolding. The resulting posteriors, together with priors and true values are shown in figure 6.2.

The plotted priors and posteriors are histograms consisting of samples from their respective distributions, and we may combine both bins to show the complete 2-dimensional histograms with 1 bin per axis. The complete prior is shown in figure 6.3. Next, we plot our 2-dimensional Poisson distribution in the truth-bin space and see that it belongs to the same domain as the combined prior. This is shown in figure 6.4.

With these pieces in place we can examine whether our Poisson distribution corresponds to the likelihood that is built into PyFBU. We do this by combining the posteriors in the same way we did the priors and plot this together with the Poisson distribution,
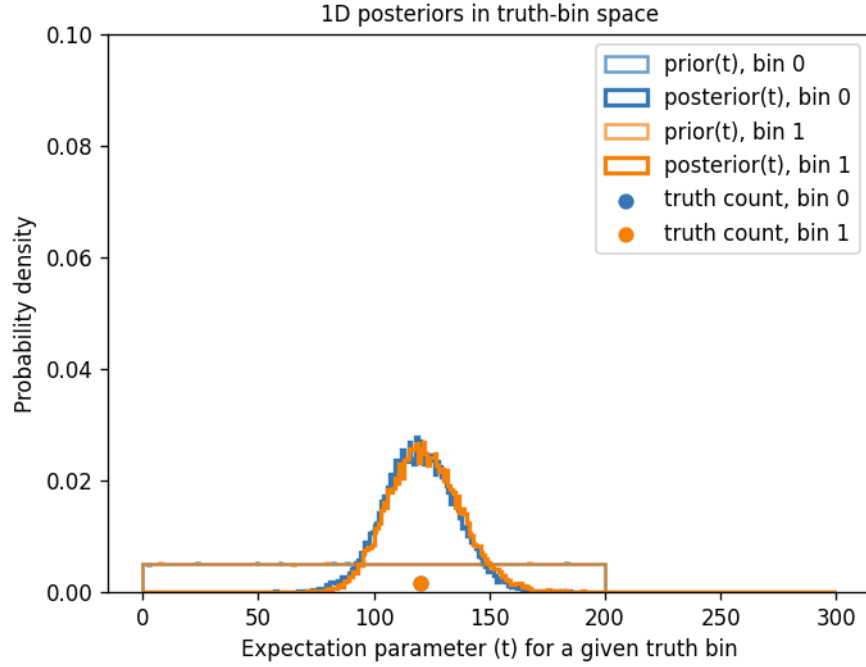
Figure 6.2: Prosterior distributions after unfolding a 2-bin constructed spectrum, along with corresponding priors and true values. Both posteriors point to the true value being located around 120, which is correct. The spread of the posteriors represents the uncertainty. We can also see that our uniform priors were suitable choices, as the true values are located within, and the posteriors are not truncated.
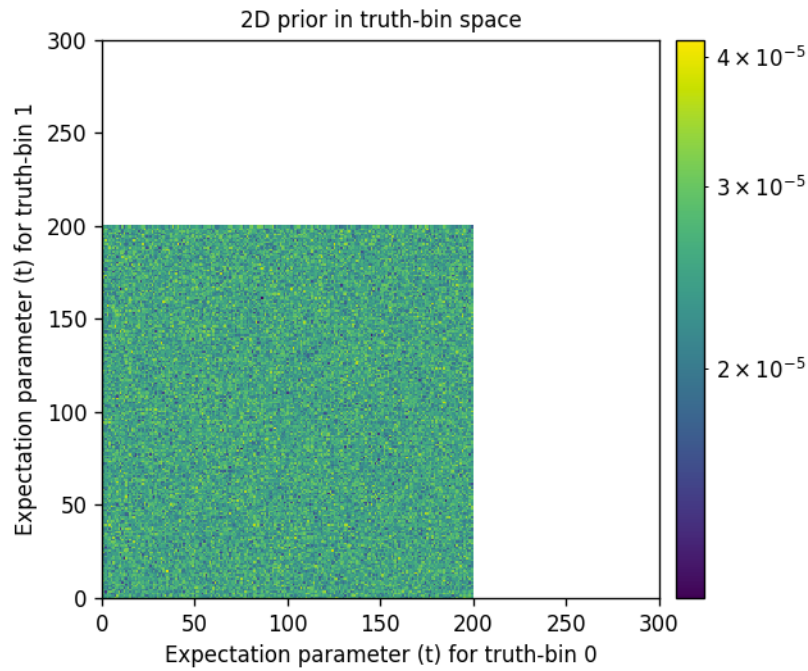

Figure 6.3: 2-dimensional complete prior distribution for both bins in the spectrum, consisting of random samples from the uniform distribution in the range $[0, 200]$.
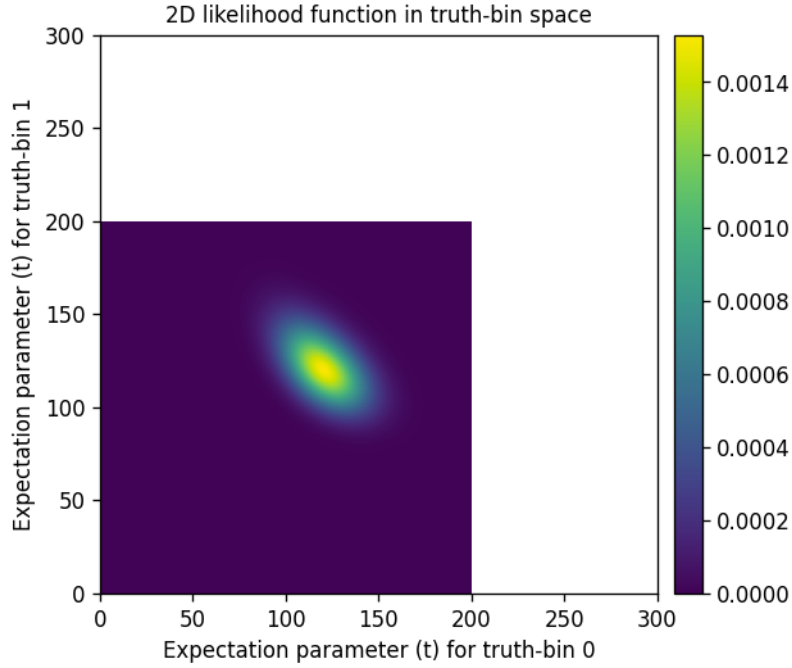
Figure 6.4: 2-dimensional Poisson distribution in the truth-bin space, dependent on the observed data and our defined ranges of possible true values. Note that this, as opposed to the prior and posterior, is a function defined over both dimensions, rather than a collection of samples.

shown in figure 6.5.

We see that our assumption about the likelihood was correct, and we have gained a stronger understanding of how the PyFBU-package is built up. This reduction of the black-box trait lets us have a greater confidence in future results, and how they actually are produced. Next, in figures 6.6 - 6.9, we examine the corresponding plots of the distributions in the folded-bin space, i.e. the space where the observed data is contained. This is where the likelihood function is originally defined, i.e. being dependent on the variable f_r in eq. 3.9 and eq. 3.8, and we will see the effect of the response matrix on the prior and posterior.
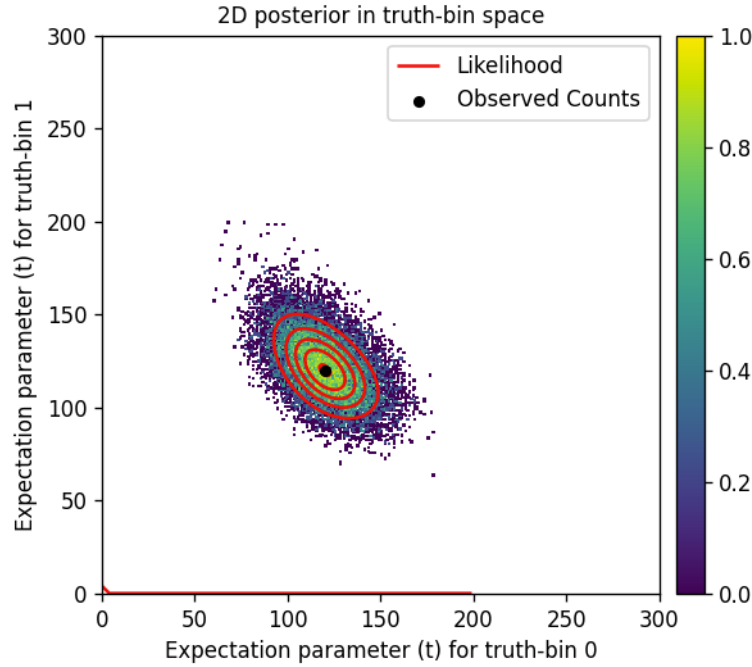
Figure 6.5: 2-dimensional complete posterior distribution for both bins, output from PyFBU, as well as contour lines from the 2-dimensional Poisson distribution shown in figure 6.4. Remember that the contours belong to a function we have defined based only on our available data and assumptions, meaning there is no connection to PyFBU. Yet, the contours exhibit a similar shape and location of the Poisson distribution as the posterior, indicating that our externally constructed function matches the internal likelihood of PyFBU. As mentioned in part II, subsection 3.3, we strictly have to compare the posterior with Poisson×prior. However, since our prior is a uniform distribution, neither the shape nor the location of the posterior is affected by the prior, meaning we can directly compare with the likelihood candidate.
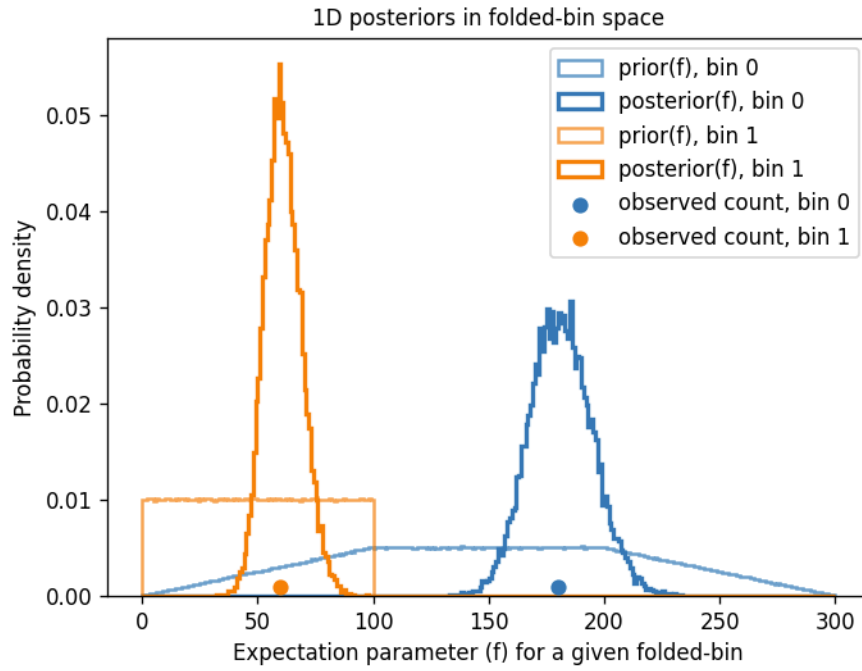
Figure 6.6: Posterior and prior distributions from figure 6.2 folded with the response matrix, along with the observed data, in folded-bin space. We see the smearing effect, how counts can be redistributed due to the detector response. The range for the prior for bin 0 is seen to have been resized from $[0, 200]$ to $[0, 300]$, and to $[0, 100]$ for bin 1. The corresponding heights have thus changed, preserving the total probability of 1 for both priors. The posteriors are centered around their respective observed counts, and show the spread for which possible observed values can lead to the true counts of 120 in this case.
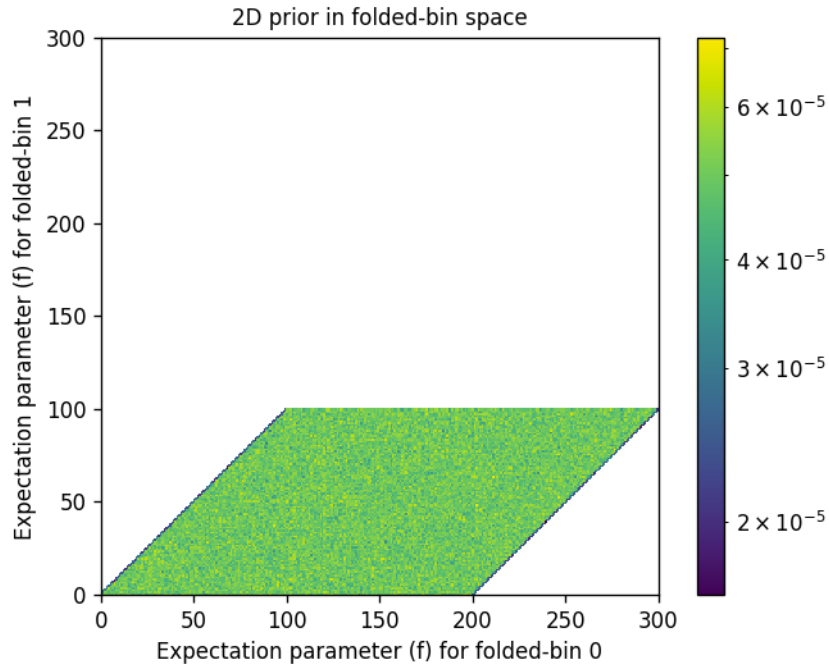
Figure 6.7: The complete 2-dimensional prior distribution from figure 6.3 in folded-bin space. We see that the prior has been skewed and occupies a smaller area than in the truth-bin space. We can also see that the prior heights, shown in color, are larger to compensate.
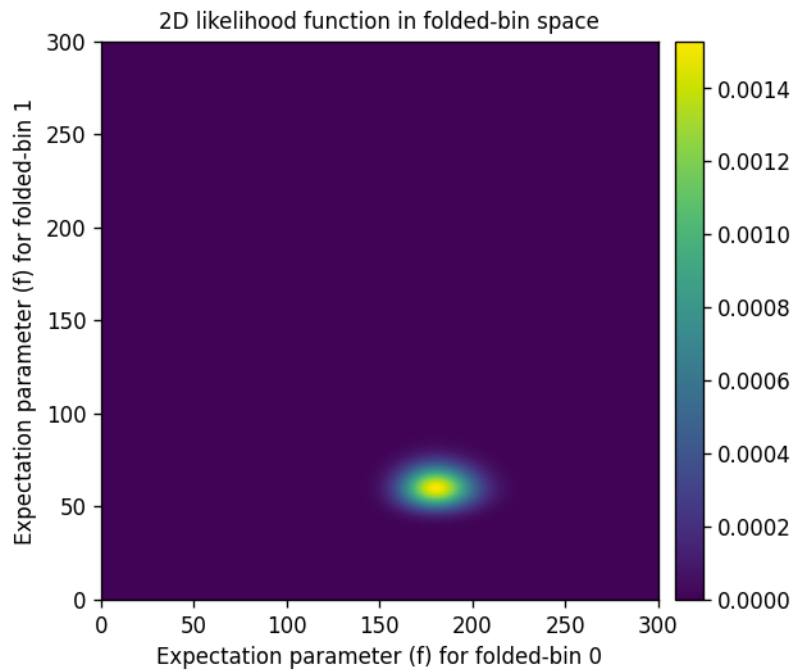

Figure 6.8: The 2-dimensional Poisson distribution from figure 6.4 in the folded-bin space, corresponding to the likelihood in PyFBU. We see a more concentrated peak here than in the truth space.
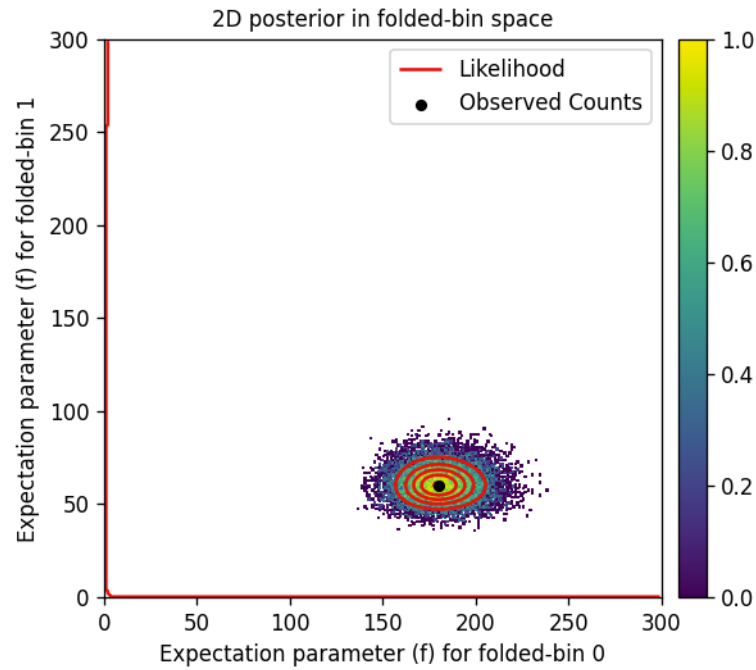
Figure 6.9: The 2-dimensional complete posterior distribution from figure 6.5, as well as contour lines from the likelihood function, in folded space. Here too, the likelihood and posterior shapes and locations match very well, confirming again our assumption about the likelihood. The narrower distribution, especially for bin 1, shows that there are less possible observed counts leading to a truth count of 120, than possible truth counts leading to the observed value from the detector.

Experimental spectra

1   28 Si spectrum

- Compare result with Valas, using logscale prior, modified likelihood?

- Background?

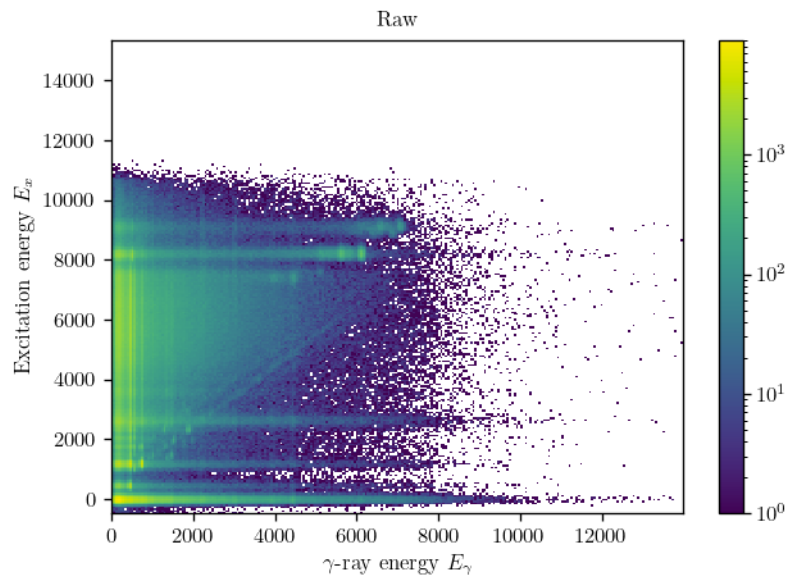## 2   146Nd

- Raw? 2 dim and projected

Figure 7.1: Complete raw spectrum for ^{146}Nd, showing the γ-ray spectra for each excitation energy E_x.
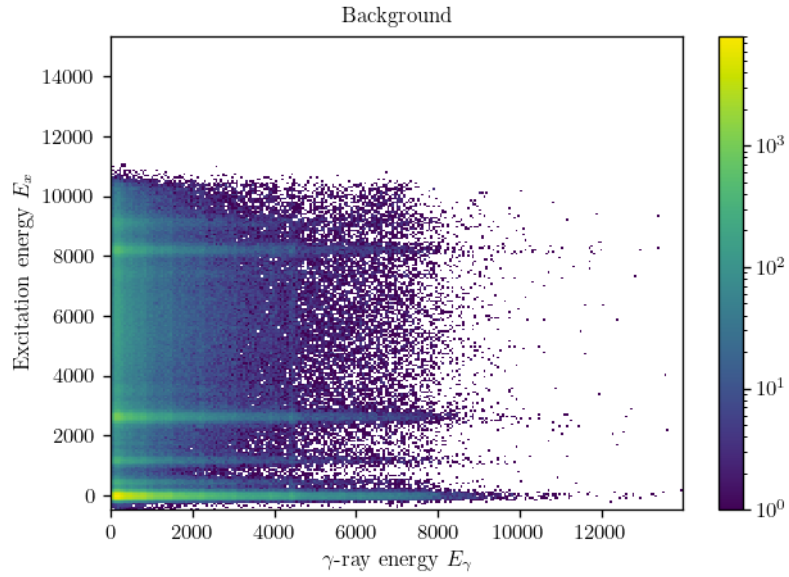
Figure 7.2: The background energies present in the raw data in figure 7.1.
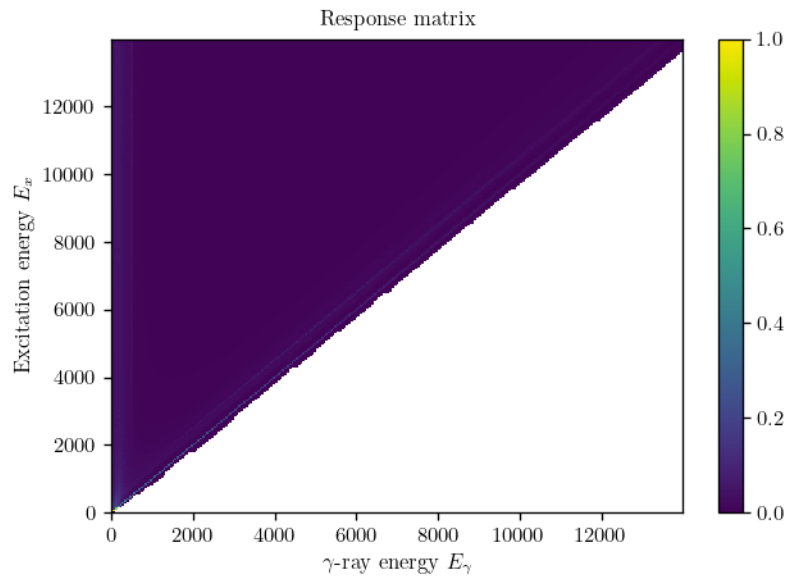
- Response?

Figure 7.3: The complete response matrix for the entire energy range

- FBU unfolded

- FBU refolded

- Residuals

- MSE, R2

- OMPY unfolded

- OMPY refolded

- residuals?

- MSE, R2

Part V

Conclusion

Bibliography

1. D. S. Sivia, J. S. *Data analysis: A Bayesian Tutorial* 2nd ed. ISBN: 0–19–856831–2 (Oxford University Press, Great Clarendon Street, Oxford OX2 6DP, 2006).

2. Cowan, G. *A survey of unfolding methods for particle physics* in *Prepared for Conference on Advanced Statistical Techniques in Particle Physics, Durham, England* (2002), 18–22.

3. Guttormsen, M., Tveter, T., Bergholt, L., Ingebretsen, F. & Rekstad, J. The unfolding of continuum γ-ray spectra. *Nuclear instruments & methods in physics research. Section A, Accelerators, spectrometers, detectors and associated equipment* **374,** 371–376. ISSN: 0168-9002 (1996).

4. Hoffman, M. D. & Gelman, A. *The No-U-Turn Sampler: Adaptively Setting Path Lengths in Hamiltonian Monte Carlo* 2011. arXiv: 1111.4246 [stat.CO].

5. Salvatier, J., Wiecki, T. V. & Fonnesbeck, C. Probabilistic programming in Python using PyMC3. *PeerJ Computer Science* **2.** Publisher: PeerJ Inc., e55. ISSN: 2376-5992. https://peerj.com/articles/cs-55 (2021) (Apr. 6, 2016).

6. Kucukelbir, A., Ranganath, R., Gelman, A. & Blei, D. M. *Automatic Variational Inference in Stan* 2015. arXiv: 1506.03431 [stat.ML].

7. Jaynes, E. T. *Probability Theory: The Logic of Science* (ed Bretthorst, G. L.) (Cambridge University Press, 2003).

8. Lee, P. M. *Bayesian statistics : an introduction* eng. Chichester, West Sussex ; 2012.

9. Edwards, W., Lindman, H. & Savage, L. J. Bayesian statistical inference for psychological research. *Psychological Review* **70.** Publisher: US: American Psychological Association, 193. ISSN: 1939-1471. http://psycnet.apa.org/fulltext/1964-00040-001.pdf (1964).

10. Valsdóttir, V. M. *Exploring Fully Bayesian Unfolding for γ-ray Spectra* MA thesis (University of Oslo, Oslo, 2020).

11. Valsdóttir, V. M. *Exploring Fully Bayesian Unfolding for γ-ray Spectra - GitHub repository* `https://github.com/valamaria89/Exploring-Fully-Bayesian-Unfolding-for-gamma-ray-Spectra` (2020).

12. Gerbaudo, D., Helsens, C. & Rubbo, F. *PyFBU* `https://github.com/pyFBU/fbu`.